epileptic encephalopathy (49) but *CBL* has not. It has been implicated as a cause of juvenile myelomonocytic leukemia (57,58) and also of a Noonan-like syndrome with microcephaly (57,59). A clinical review after our discovery confirmed that Patient 6 did not have facial features typical of Noonan syndrome. Thus, our results suggest that *CBL* mutations may give rise to an even wider spectrum of phenotypes than previously thought.

Our discovery of the *de novo* non-synonymous *CSNK1G1* mutation in Patient 5 hints that the epileptogenic mechanism may involve the Wnt pathway, which CK1 regulates (60,61), although disruptions in synaptic transmission due to abnormal phosphorylation of NMDA receptors (45) would be a more direct explanation. Intriguingly, the *Drosophila* homolog of *CSNK1G3* was found to suppress seizures in the Na^+-channel gain-of-function mutant $para^{bss1}$ (62). Also, a mutation in *PRICKLE1*, which encodes a regulator of the Dishevelled proteins that are intracellular transducers of Wnt signals (63), has been reported to cause progressive myoclonic epilepsy (61). For both *CBL* and *CSNK1G1*, causality can only be definitely established by finding other mutations in patients with similar phenotypes or by extensive functional work in model organisms. Identifying and screening cases similar to Patient 6, rather than those with a more typical NCFC clinical presentation, may increase the chance of finding further patients with *CBL* mutations.

Other groups have already demonstrated the power of WES and WGS in rapidly pinpointing novel genes underlying a rare disease (1,64), particularly in the case of *de novo* inheritance (65). Although all the cases described in this article could probably have been solved by WES, which would have been considerably cheaper, there is emerging evidence to suggest that WES misses clinically relevant mutations because of unequal or incomplete coverage of exons, particularly around the exon boundaries (66). Given that two of our mutations were in splice sites, this was especially relevant. Additionally, the ability to check for pathogenic non-coding mutations in WGS data, as we have done around known early-onset epilepsy genes, is an additional benefit of this approach.

Our study underlines the significant potential of WGS for providing rapid clinical diagnosis of patients with heterogeneous genetic diseases. The patients being investigated here had undergone numerous genetic, biochemical and imaging tests over many years but had been refractory to diagnosis. Using WGS, three of the six patients (Patients 1–3) received a confirmed molecular diagnosis in a clinically relevant timeframe. Conventional molecular testing would not have included these genes. *KCNT1* had not previously been implicated in OS and would not therefore have been tested for this specific phenotype, even though it was described for other severe epilepsy phenotypes after we started this project (29,31). Similarly, *KCNQ2* and *SCN2A* had only been described for benign seizures (67,68) until recent reports of association with the more severe OS phenotype (17,18). These results have already improved the clinical management of these patients' families by providing informed and accurate reproductive risk counseling and the prospect of prenatal diagnosis for future pregnancies.

For the remaining three patients, candidate mutations likely to cause their epilepsy have been identified. The evidence is particularly strong for *PIGQ*, since a homozygous nonsense mutation in *PIGA* causes a similar phenotype (35), and we demonstrated that our mutation was loss of function. Further genetic and functional validation work is required to prove causality definitively, and this remains a challenge in a clinical setting, particularly for rare diseases. Nevertheless, this situation is expected to improve with greater adoption of these technologies and increased sharing of genetic data in public databases.

In conclusion, our results have led to identification of novel genes for severe epilepsy phenotypes and, in addition, demonstrate the clinical utility of WGS as a means of providing comprehensive and rapid molecular diagnosis for patients with mechanistically complex genetic diseases, with concomitant implications for clinical management of these disorders.

MATERIALS AND METHODS

Description of patients

The six patients were recruited through the Oxford Clinical Genetics department. A summary of the main clinical features is given in Table 1, along with a list of the genetic tests they had undergone before entering this study (all of which were negative). All patients also had extensive metabolic tests on blood, urine and cerebral spinal fluid, all of which were normal. A more detailed clinical description is given in Supplementary Materials, Note S1.

Read mapping and variant calling

WGS was conducted on the Illumina HiSeq platform to a coverage of at least 25×. The reads were mapped to the human reference genome (build 37d5) with Stampy (69), and SNVs and small indels were called with an in-house algorithm, Platypus (70). Variants were annotated relative to RefSeq transcripts using ANNOVAR (71) and relative to all Ensembl transcripts using an in-house tool called VariantAnno.

Variant filtering strategy

To identify *de novo* mutations in the trios, we first screened for variants that were called as homozygous reference in the parents but heterozygous in the child. We then filtered these based on the genotype likelihood ratio (the difference between the log likelihoods for the most likely and the second most likely genotypes), requiring this to be below −5 in all three individuals. This left an average of 126 candidate *de novo* mutations in each trio [about 70 being expected given a mutation rate of 1.18×10^{-8} per base pair per generation (72)]. To remove those likely to be due to technical artifacts or incorrect calling of parental genotypes, we removed variants that had been seen before in WGS500, the 1000 Genomes Project or the NHLBI Exome Sequencing Project (ESP). We then prioritized variants that were predicted to alter the protein sequence in any transcript (non-synonymous SNVs, stop loss or gain variants, indels or splice site mutations), particularly those that were highly conserved across the 46 vertebrate species in the UCSC conservation track. There were 0–3 candidate *de novo* coding mutations per trio.

We also considered a simple recessive or compound heterozygous model in all families, as well as an X-linked model where appropriate. For the compound heterozygous model, we required

two coding variants in the same gene, one inherited from each heterozygous parent. Since EOEE is extremely rare (frequency ~1/100 000), we excluded variants with a frequency greater than 0.005 in 1000 Genomes or ESP, or for which there were any homozygotes or hemizygotes or more than five heterozygotes among the other WGS500 samples ($n = 294$), which included no other patients with seizures.

In addition to screening for coding variants, we also looked for variants that might be affecting regulation of known EOEE genes. Specifically, we focused on variants at conserved positions in regulatory regions within 50 kb of the candidate genes *KCNQ2, SCN2A, SCN1A, SPTAN1, SRGAP2, MAGI1, PLCB1, STXBP1, PNPO, PCDH19, GRIN2A, MAPK10, CDKL5, SLC25A22, ERBB4* and *ARX*. A variant was considered conserved if it had a GERP (73) or phyloP (74) score greater than 2 or a phastCons (75) score greater than 0.95, or was in a GERP constrained element (73) or a phastCons constrained element (75). We used the regulatory regions defined by the Ensembl V65 Regulatory Build (http://www.ensembl.org/info/genome/funcgen/regulatory_build.html, last accessed date on February, 2013).

Variant validation

All putatively causal variants were Sanger-sequenced to confirm the genotypes of the proband and parents.

Splicing assays

Fresh blood was collected using PAXgene blood RNA tubes (Becton Dickinson, Oxford, UK) and RNA was extracted using the PAXgene Blood RNA kit (Qiagen). cDNA was synthesized using the QuantiTect Reverse Transcription kit (Qiagen) according to the manufacturer's instructions. We carried out a PCR using the FastStart Kit (Roche) and primers as follows: PIGQ-2F, CACGCAGTGAGGTGCTCTT; PIGQ-5R, GGGG ACATGAGGTGGATGTA; CBL-8F, GAGATGGGCTCCA CATTCC; CBL-11R, GAACTTGGGGCAGATACTGG. To size PCR products accurately, we used 'on-chip-electrophoresis' and ran 1 μl on a DNA 1000 v2.3 chip using the 2100 Bioanalyser system (Agilent). We expected WT RT-PCR products of 583 and 698 bp for NM_004204 (*PIGQ*) and NM_005188 (*CBL*), respectively. Sanger sequencing was used to confirm the identity of the aberrant bands.

KCNT1 functional work

Site-directed mutagenesis and cRNA synthesis

The rat homologue (A945T) of the human *KCNT1* A966T mutation was created using the QuikChange Mutagenesis kit (Stratagene) using the WT *KCNT1* construct in pOX expression vector as the template, and the following primers: 5′-GTTCCGCCT GCCATTTGCTACTGGTCGGGTGTTTAGTA-3′ (forward) and 5′-TACTAAACACCCGACCAGTAGCAAATGGCAGG CGGAAC-3′ (reverse). The resulting construct was sequenced to confirm the presence of mutation. The cDNA construct was then linearized using NotI, and the complementary RNA (cRNA) made using the mMessage mMachine T3 kit (Ambion). The final reaction was purified using MinElute PCR Purification kit (Qiagen), and RNA eluted in nuclease-free water. RNA purity and concentration was checked using a NanoDrop reader. RNA quality was also checked on a 1% formaldehyde agarose gel, and its densitometry quantitated using ImageJ to confirm its concentration. cRNA was stored at −20°C until ready for use.

Electrophysiological characterization in Xenopus laevis *oocytes*

All animal procedures were approved by the IACUC at Yale University. Oocytes were prepared as described previously (31). Defolliculated oocytes were injected with 10 ng of RNA encoding WT or A966T, or with sterile water. Oocytes were kept at 18°C, and two-electrode voltage clamping was performed on days 2–5 post-injection, as reported previously (31,76).

PIGQ functional work

We used a previously described human *PIGQ* expression vector (77). The *PIGQ* mutant construct lacking exon 3 was made by site-directed mutagenesis. *PIGQ*-deficient CHO cells (10.2.1) (78) were transiently transfected with FLAG-tagged WT or mutant *PIGQ* cDNA, driven by an SRα promoter (pME FLAG-PIGQ) together with a luciferase expression plasmid for monitoring transfection efficiency. Two days later, to determine the restoration of GPI-AP expression, cells were stained with anti-CD59 (5H8) antibody followed by phycoerythrin-conjugated anti-mouse IgG, and analyzed by a flow cytometer (Cant II; BD Biosciences, Franklin Lakes, NJ, USA) using the Flowjo software (Tommy Digital Inc., Tokyo, Japan). To determine FLAG-tagged *PIGQ* protein levels, lysates of transfected cells were subjected to SDS–PAGE, and western blotting was performed using anti-FLAG antibody (M2, Sigma, St Louis, MO, USA), with anti-GAPDH (6C5, Life Technologies, Carlsbad, CA, USA) as a loading control. Transfection efficiency was determined by luciferase activity using the Luciferase assay kit (Promega, Madison, WI, USA).

Screening candidate genes in Australian cohort

We sequenced *PIGQ*, *CSNK1G1*, *CBL* and *KCNT1* in a cohort of 500 epileptic encephalopathy patients from Australia. These patients had a variety of different phenotypes, the breakdown of which is shown in Supplementary Materials, Table S1, with an age of onset ranging from 1 day to 25 years.

We used Molecular Inversion Probes (MIPs) to capture all exon and intron/exon boundaries (5 bp flanking) of target genes (Refseq, hg19 build). Detailed methodology is described elsewhere (79). Briefly, pooled MIPs (Supplementary Materials, Table S3) were used to capture target exons from 100 ng of each proband's DNA and target enrichment was performed by PCR using unique reverse primers for each DNA sample. Pooled libraries were subject to massively parallel sequencing using a 101 paired-end protocol on a HiSeq.

We performed raw read processing as described (79), but use a modified analysis pipeline for variant calling. SNV and indel calling and filtering was performed using the Genome Analysis Tool Kit (GATK version 2.2) (http://www.broadinstitute.org/gatk/, last accessed date on February, 2013). We excluded from further analysis any variants with allele balance >0.70,

QUAL < 30, QD < 5 or coverage < 25×, and variants in clusters (window size 10 bp) or in homopolymer runs (5 bp). Variants were annotated with SeattleSeq (version 134; http://snp.gs.washington.edu/SeattleSeqAnnotation134/) and the Exome Sequencing Project dataset (see http://eversusgs.washington.edu/EVS/, last accessed date on February, 2013) used to assess variant frequency in the control population. For dominant (or *de novo*) models, we considered only variants not present in this control sample set. For recessive candidates, we considered variants with a frequency in controls of <1% (European American control frequency). Only non-synonymous, splice-site or frameshift variants were assessed further.

Where family members were available, segregation analysis was performed using a 'MIP-pick' strategy. We selected and re-pooled only the MIPs that captured the genomic sequence harboring the rare variant of interest and performed target enrichment PCR and sequencing as above for all relevant probands and family members.

Screening candidate genes in UK cases

We carried out Sanger sequencing of *CBL*, *CSNK1G1*, *PIGQ* and *KCNT1* in 11 patients with Ohtahara syndrome. Clinical details are given in Supplementary Materials, Table S2. Genomic DNA from participating individuals was extracted from peripheral lymphocytes by standard techniques. All participants gave written informed consent and the study was performed in accordance with the Declaration of Helsinki.

Primer pairs were designed for all coding exons with primer3 software (1,2) (http://bioinfo.ut.ee/primer3/, last accessed date on February, 2013) (Supplementary Materials, Table S4). The exons were amplified by PCR using BioMix™ Red (Bioline Ltd). Two different PCR conditions were carried out to amplify exons: (i) an initial denaturation of 95°C for 5 min, followed by 35 cycles of 45 s denaturation at 95°C, 45 s annealing at 58–62°C (depending on fragment) and 1 min extension at 72°C with a final extension at 72°C for 5 min, or (ii) a touchdown PCR program: an initial denaturation of 95°C for 5 min, followed by 24 cycles of 30 s denaturation at 95°C, 30 s annealing at 62°C (minus 0.5°C per cycle) and 1 min extension at 72°C, followed by 15 cycles of 30 s denaturation at 95°C, 30 s annealing at 50°C and 1 min extension at 72°C with a final extension at 72°C for 10 min. If PCR condition 1 was not successful, PCR condition 2 was applied. PCR products were cleaned up with MicroCLEAN (Web Scientific) and were directly sequenced by the Big Dye Terminator Cycle Sequencing System (Applied Biosystems Inc.). Sequencing reactions were run on an ABI PRISM 3730 DNA Analyzer (Applied Biosystems Inc.) and analyzed using Chromas (http://www.technelysium.com.au/chromas.html, last accessed date on February, 2013).

AUTHOR CONTRIBUTIONS

H.C.M. analyzed the WGS data. L.K.K. directed the *KCNT1* electrophysiology experiments, which were performed by G.E.K., M.F., M.R.B. and J.K. A.T.P. and K.A.H. did the Sanger sequencing and splicing assays. G.B. made the *KCNT1* construct for electrophysiology, supervised by R.N. J.B., A.K. and J.-B.C. created the bioinformatics infrastructure of the WGS500 project and provided NGS data processing, preparing the BAM files and variant calls. R.C. and A.R. contributed to WGS analysis. Y.M. and T.K. did the *in vitro PIGQ* experiments. S.H. and I.E.S. studied patients in the Australian cohort and performed phenotyping analysis of the larger epilepsy panel, on which G.C. and H.M. performed the MIP sequencing. M.A.K. and E.M. performed phenotyping and Sanger sequencing on the UK cohort. H.S., D.S. and E.B. contributed samples and clinical data from the affected individuals and assisted with the interpretation of results. Z.Z. and T.M. provided clinical data and advice on the phenotypes. E.B., D.B., G.M., J.C.T. and P.D. conceived the study, and L.K.K., E.B., P.D. and J.T. directed it. H.C.M., G.E.K., A.T.P., E.B., I.E.S., L.K.K., J.C.T. and P.D. wrote the article. This project was carried out as part of the WGS500 Consortium.

SUPPLEMENTARY MATERIAL

Supplementary Material is available at *HMG* online.

ACKNOWLEDGEMENTS

We thank the patients and their families for participating in this study, the Genomics Core at the Wellcome Trust Centre for Human Genetics (WTCHG) for generating the WGS data, Elham Sadighi Akha for running the SNP arrays for trio 2 and Kevin Leyden for doing the CD59 flow cytometry assay for trio 4. We are also grateful to Adeline Nogh and Amy McTague for their input in gathering the UCL cohort, and to Helen Cross and Jozef Gecz for facilitating initial contact between groups.

Conflict of Interest statement. D.B. is an employee of Illumina Inc.

FUNDING

This work was supported in part by a Wellcome Trust Core Award (090532/Z/09/Z) to the Wellcome Trust Centre for Human Genetics and a Wellcome Trust Senior Investigator Award to P.D. (095552/2/11/2), in part by NIH grant HD067517 and in part by the Oxford NIHR Biomedical Research Centre. Funding to pay the Open Access publication charges for this article was provided by the wellcome Trust and the Oxford NIHR Biomedical Research Centre.

REFERENCES

1. Bamshad, M.J., Ng, S.B., Bigham, A.W., Tabor, H.K., Emond, M.J., Nickerson, D.A. and Shendure, J. (2011) Exome sequencing as a tool for Mendelian disease gene discovery. *Nat. Rev. Genet.*, **12**, 745–755.
2. Rabbani, B., Mahdieh, N., Hosomichi, K., Nakaoka, H. and Inoue, I. (2012) Next-generation sequencing: impact of exome sequencing in characterizing Mendelian disorders. *J. Hum. Genet.*, **57**, 621–632.
3. Palles, C., Cazier, J.B., Howarth, K.M., Domingo, E., Jones, A.M., Broderick, P., Kemp, Z., Spain, S.L., Almeida, E.G., Salguero, I. *et al.* (2012) Germline mutations affecting the proofreading domains of POLE and POLD1 predispose to colorectal adenomas and carcinomas. *Nat. Genet.*, **45**, 136–144.
4. Lise, S., Clarkson, Y., Perkins, E., Kwasniewska, A., Sadighi Akha, E., Schnekenberg, R.P., Suminaite, D., Hope, J., Baker, I., Gregory, L. *et al.*

(2012) Recessive mutations in SPTBN2 implicate beta-III spectrin in both cognitive and motor development. *PLoS Genet.*, **8**, e1003074.
5. Sharma, V.P., Fenwick, A.L., Brockop, M.S., McGowan, S.J., Goos, J.A., Hoogeboom, A.J., Brady, A.F., Jeelani, N.O., Lynch, S.A., Mulliken, J.B. *et al.* (2013) Mutations in TCF12, encoding a basic helix-loop-helix partner of TWIST1, are a frequent cause of coronal craniosynostosis. *Nat. Genet.*, **45**, 304–307.
6. Nordli, D.R. Jr. (2012) Epileptic encephalopathies in infants and children. *J. Clin. Neurophysiol.*, **29**, 420–424.
7. Kodera, H., Kato, M., Nord, A.S., Walsh, T., Lee, M., Yamanaka, G., Tohyama, J., Nakamura, K., Nakagawa, E., Ikeda, T. *et al.* (2013) Targeted capture and sequencing for detection of mutations causing early onset epileptic encephalopathy. *Epilepsia*, **54**, 1262–1269.
8. Berg, A.T., Berkovic, S.F., Brodie, M.J., Buchhalter, J., Cross, J.H., van Emde Boas, W., Engel, J., French, J., Glauser, T.A., Mathern, G.W. *et al.* (2010) Revised terminology and concepts for organization of seizures and epilepsies: report of the ILAE Commission on Classification and Terminology, 2005–2009. *Epilepsia*, **51**, 676–685.
9. Ohtahara, S. and Yamatogi, Y. (2003) Epileptic encephalopathies in early infancy with suppression-burst. *J. Clin. Neurophysiol.*, **20**, 398–407.
10. Pavone, P., Spalice, A., Polizzi, A., Parisi, P. and Ruggieri, M. (2012) Ohtahara syndrome with emphasis on recent genetic discovery. *Brain Dev.*, **34**, 459–468.
11. Hino-Fukuyo, N., Haginoya, K., Iinuma, K., Uematsu, M. and Tsuchiya, S. (2009) Neuroepidemiology of West syndrome and early infantile epileptic encephalopathy in Miyagi Prefecture, Japan. *Epilepsy Res.*, **87**, 299–301.
12. Tavyev Asher, Y.J. and Scaglia, F. (2012) Molecular bases and clinical spectrum of early infantile epileptic encephalopathies. *Eur. J. Med. Genet.*, **55**, 299–306.
13. Kato, M., Saitoh, S., Kamei, A., Shiraishi, H., Ueda, Y., Akasaka, M., Tohyama, J., Akasaka, N. and Hayasaka, K. (2007) A longer polyalanine expansion mutation in the ARX gene causes early infantile epileptic encephalopathy with suppression-burst pattern (Ohtahara syndrome). *Am. J. Hum. Genet.*, **81**, 361–366.
14. Saitsu, H., Kato, M., Mizuguchi, T., Hamada, K., Osaka, H., Tohyama, J., Uruno, K., Kumada, S., Nishiyama, K., Nishimura, A. *et al.* (2008) De novo mutations in the gene encoding STXBP1 (MUNC18–1) cause early infantile epileptic encephalopathy. *Nat. Genet.*, **40**, 782–788.
15. Deprez, L., Weckhuysen, S., Holmgren, P., Suls, A., Van Dyck, T., Goossens, D., Del-Favero, J., Jansen, A., Verhaert, K., Lagae, L. *et al.* (2010) Clinical spectrum of early-onset epileptic encephalopathies associated with STXBP1 mutations. *Neurology*, **75**, 1159–1165.
16. Melani, F., Mei, D., Pisano, T., Savasta, S., Franzoni, E., Ferrari, A.R., Marini, C. and Guerrini, R. (2011) CDKL5 gene-related epileptic encephalopathy: electroclinical findings in the first year of life. *Dev. Med. Child Neurol.*, **53**, 354–360.
17. Saitsu, H., Kato, M., Koide, A., Goto, T., Fujita, T., Nishiyama, K., Tsurusaki, Y., Doi, H., Miyake, N., Hayasaka, K. *et al.* (2012) Whole exome sequencing identifies KCNQ2 mutations in Ohtahara syndrome. *Ann. Neurol.*, **72**, 298–300.
18. Nakamura, K., Kato, M., Osaka, H., Yamashita, S., Nakagawa, E., Haginoya, K., Tohyama, J., Okuda, M., Wada, T., Shimakawa, S. *et al.* (2013) Clinical spectrum of SCN2A mutations expanding to Ohtahara syndrome. *Neurology*, **81**, 992–998.
19. Touma, M., Joshi, M., Connolly, M.C., Grant, P.E., Hansen, A.R., Khwaja, O., Berry, G.T., Kinney, H.C., Poduri, A. and Agrawal, P.B. (2013) Whole genome sequencing identifies SCN2A mutation in monozygotic twins with Ohtahara syndrome and unique neuropathologic findings. *Epilepsia*, **54**, e81–e85.
20. Veeramah, K.R., O'Brien, J.E., Meisler, M.H., Cheng, X., Dib-Hajj, S.D., Waxman, S.G., Talwar, D., Girirajan, S., Eichler, E.E., Restifo, L.L. *et al.* (2012) De novo pathogenic SCN8A mutation identified by whole-genome sequencing of a family quartet affected by infantile epileptic encephalopathy and SUDEP. *Am. J. Hum. Genet.*, **90**, 502–510.
21. Molinari, F., Raas-Rothschild, A., Rio, M., Fiermonte, G., Encha-Razavi, F., Palmieri, L., Palmieri, F., Ben-Neriah, Z., Kadhom, N., Vekemans, M. *et al.* (2005) Impaired mitochondrial glutamate transport in autosomal recessive neonatal myoclonic epilepsy. *Am. J. Hum. Genet.*, **76**, 334–339.
22. Saitsu, H., Tohyama, J., Kumada, T., Egawa, K., Hamada, K., Okada, I., Mizuguchi, T., Osaka, H., Miyata, R., Furukawa, T. *et al.* (2010) Dominant-negative mutations in alpha-II spectrin cause West syndrome with severe cerebral hypomyelination, spastic quadriplegia, and developmental delay. *Am. J. Hum. Genet.*, **86**, 881–891.
23. Kurian, M.A., Meyer, E., Vassallo, G., Morgan, N.V., Prakash, N., Pasha, S., Hai, N.A., Shuib, S., Rahman, F., Wassmer, E. *et al.* (2010) Phospholipase C beta 1 deficiency is associated with early-onset epileptic encephalopathy. *Brain*, **133**, 2964–2970.
24. Shen, J., Gilmore, E.C., Marshall, C.A., Haddadin, M., Reynolds, J.J., Eyaid, W., Bodell, A., Barry, B., Gleason, D., Allen, K. *et al.* (2010) Mutations in PNKP cause microcephaly, seizures and defects in DNA repair. *Nat. Genet.*, **42**, 245–249.
25. Mills, P.B., Surtees, R.A., Champion, M.P., Beesley, C.E., Dalton, N., Scambler, P.J., Heales, S.J., Briddon, A., Scheimberg, I., Hoffmann, G.F. *et al.* (2005) Neonatal epileptic encephalopathy caused by mutations in the PNPO gene encoding pyridox(am)ine 5′-phosphate oxidase. *Hum. Mol. Genet.*, **14**, 1077–1086.
26. Weckhuysen, S., Mandelstam, S., Suls, A., Audenaert, D., Deconinck, T., Claes, L.R., Deprez, L., Smets, K., Hristova, D., Yordanova, I. *et al.* (2012) KCNQ2 encephalopathy: emerging phenotype of a neonatal epileptic encephalopathy. *Ann. Neurol.*, **71**, 15–25.
27. Laezza, F., Lampert, A., Kozel, M.A., Gerber, B.R., Rush, A.M., Nerbonne, J.M., Waxman, S.G., Dib-Hajj, S.D. and Ornitz, D.M. (2009) FGF14 N-terminal splice variants differentially modulate Nav1.2 and Nav1.6-encoded sodium channels. *Mol. Cell. Neurosci.*, **42**, 90–101.
28. Bhattacharjee, A., Gan, L. and Kaczmarek, L.K. (2002) Localization of the Slack potassium channel in the rat central nervous system. *J. Comp. Neurol.*, **454**, 241–254.
29. Heron, S.E., Smith, K.R., Bahlo, M., Nobili, L., Kahana, E., Licchetta, L., Oliver, K.L., Mazarib, A., Afawi, Z., Korczyn, A. *et al.* (2012) Missense mutations in the sodium-gated potassium channel gene KCNT1 cause severe autosomal dominant nocturnal frontal lobe epilepsy. *Nat. Genet.*, **44**, 1188–1190.
30. McTague, A., Appleton, R., Avula, S., Cross, J.H., King, M.D., Jacques, T.S., Bhate, S., Cronin, A., Curran, A., Desurkar, A. *et al.* (2013) Migrating partial seizures of infancy: expansion of the electroclinical, radiological and pathological disease spectrum. *Brain*, **136**, 1578–1591.
31. Barcia, G., Fleming, M.R., Deligniere, A., Gazula, V.R., Brown, M.R., Langouet, M., Chen, H., Kronengold, J., Abhyankar, A., Cilio, R. *et al.* (2012) De novo gain-of-function KCNT1 channel mutations cause malignant migrating partial seizures of infancy. *Nat. Genet.*, **44**, 1255–1259.
32. Allen, A.S., Berkovic, S.F., Cossette, P., Delanty, N., Dlugos, D., Eichler, E.E., Epstein, M.P., Glauser, T., Goldstein, D.B., Han, Y. *et al.* (2013) De novo mutations in epileptic encephalopathies. *Nature*, **501**, 217–221.
33. Joiner, W.J., Tang, M.D., Wang, L.Y., Dworetzky, S.I., Boissard, C.G., Gan, L., Gribkoff, V.K. and Kaczmarek, L.K. (1998) Formation of intermediate-conductance calcium-activated potassium channels by interaction of Slack and Slo subunits. *Nat. Neurosci.*, **1**, 462–469.
34. Hong, Y., Ohishi, K., Watanabe, R., Endo, Y., Maeda, Y. and Kinoshita, T. (1999) GPI1 stabilizes an enzyme essential in the first step of glycosylphosphatidylinositol biosynthesis. *J. Biol. Chem.*, **274**, 18582–18588.
35. Johnston, J.J., Gropman, A.L., Sapp, J.C., Teer, J.K., Martin, J.M., Liu, C.F., Yuan, X., Ye, Z., Cheng, L., Brodsky, R.A. *et al.* (2012) The phenotype of a germline mutation in PIGA: the gene somatically mutated in paroxysmal nocturnal hemoglobinuria. *Am. J. Hum. Genet.*, **90**, 295–300.
36. Maydan, G., Noyman, I., Har-Zahav, A., Neriah, Z.B., Pasmanik-Chor, M., Yeheskel, A., Albin-Kaplanski, A., Maya, I., Magal, N., Birk, E. *et al.* (2011) Multiple congenital anomalies-hypotonia-seizures syndrome is caused by a mutation in PIGN. *J. Med. Genet.*, **48**, 383–389.
37. Almeida, A.M., Murakami, Y., Layton, D.M., Hillmen, P., Sellick, G.S., Maeda, Y., Richards, S., Patterson, S., Kotsianidis, I., Mollica, L. *et al.* (2006) Hypomorphic promoter mutation in PIGM causes inherited glycosylphosphatidylinositol deficiency. *Nat. Med.*, **12**, 846–851.
38. Krawitz, P.M., Schweiger, M.R., Rodelsperger, C., Marcelis, C., Kolsch, U., Meisel, C., Stephani, F., Kinoshita, T., Murakami, Y., Bauer, S. *et al.* (2010) Identity-by-descent filtering of exome sequence data identifies PIGV mutations in hyperphosphatasia mental retardation syndrome. *Nat. Genet.*, **42**, 827–829.
39. Thompson, M.D., Roscioli, T., Marcelis, C., Nezarati, M.M., Stolte-Dijkstra, I., Sharom, F.J., Lu, P., Phillips, J.A., Sweeney, E., Robinson, P.N. *et al.* (2012) Phenotypic variability in hyperphosphatasia with seizures and neurologic deficit (Mabry syndrome). *Am. J. Med. Genet. A*, **158A**, 553–558.
40. Krawitz, P.M., Murakami, Y., Hecht, J., Kruger, U., Holder, S.E., Mortier, G.R., Delle Chiaie, B., De Baere, E., Thompson, M.D., Roscioli, T. *et al.* (2012) Mutations in PIGO, a member of the GPI-anchor-synthesis pathway,

cause hyperphosphatasia with mental retardation. *Am. J. Hum. Genet.*, **91**, 146–151.
41. Fujita, M. and Kinoshita, T. (2012) GPI-anchor remodeling: potential functions of GPI-anchors in intracellular trafficking and membrane dynamics. *Biochim. Biophys. Acta*, **1821**, 1050–1058.
42. Labasque, M. and Faivre-Sarrailh, C. (2010) GPI-anchored proteins at the node of Ranvier. *FEBS Lett.*, **584**, 1787–1792.
43. Borrie, S.C., Baeumer, B.E. and Bandtlow, C.E. (2012) The Nogo-66 receptor family in the intact and diseased CNS. *Cell Tissue Res.*, **349**, 105–117.
44. McKean, D.M. and Niswander, L. (2012) Defects in GPI biosynthesis perturb Cripto signaling during forebrain development in two new mouse models of holoprosencephaly. *Biol. Open*, **1**, 874–883.
45. Chergui, K., Svenningsson, P. and Greengard, P. (2005) Physiological role for casein kinase 1 in glutamatergic synaptic transmission. *J. Neurosci.*, **25**, 6601–6609.
46. Swaminathan, G. and Tsygankov, A.Y. (2006) The Cbl family proteins: ring leaders in regulation of cell signaling. *J. Cell. Physiol.*, **209**, 21–43.
47. Kales, S.C., Ryan, P.E., Nau, M.M. and Lipkowitz, S. (2010) Cbl and human myeloid neoplasms: the Cbl oncogene comes of age. *Cancer Res.*, **70**, 4789–4794.
48. Denayer, E. and Legius, E. (2007) What's new in the neuro-cardio-facial-cutaneous syndromes? *Eur. J. Pediatr.*, **166**, 1091–1098.
49. Adachi, M., Abe, Y., Aoki, Y. and Matsubara, Y. (2012) Epilepsy in RAS/MAPK syndrome: two cases of cardio-facio-cutaneous syndrome with epileptic encephalopathy and a literature review. *Seizure*, **21**, 55–60.
50. Carvill, G.L., Heavin, S.B., Yendle, S.C., McMahon, J.M., O'Roak, B.J., Cook, J., Khan, A., Dorschner, M.O., Weaver, M., Calvert, S. *et al.* (2013) Targeted resequencing in epileptic encephalopathies identifies de novo mutations in CHD2 and SYNGAP1. *Nat. Genet.*, **45**, 825–830.
51. Djukic, A., Lado, F.A., Shinnar, S. and Moshe, S.L. (2006) Are early myoclonic encephalopathy (EME) and the Ohtahara syndrome (EIEE) independent of each other? *Epilepsy Res.*, **70** (Suppl. 1), S68–S76.
52. Molinari, F. (2010) Mitochondria and neonatal epileptic encephalopathies with suppression burst. *J. Bioenerg. Biomembr.*, **42**, 467–471.
53. Vantaggiato, C., Redaelli, F., Falcone, S., Perrotta, C., Tonelli, A., Bondioni, S., Morbin, M., Riva, D., Saletti, V., Bonaglia, M.C. *et al.* (2009) A novel CLN8 mutation in late-infantile-onset neuronal ceroid lipofuscinosis (LINCL) reveals aspects of CLN8 neurobiological function. *Hum. Mutat.*, **30**, 1104–1116.
54. Gumus, H., Ghesquiere, S., Per, H., Kondolot, M., Ichida, K., Poyrazoglu, G., Kumandas, S., Engelen, J., Dundar, M. and Caglayan, A.O. (2010) Maternal uniparental isodisomy is responsible for serious molybdenum cofactor deficiency. *Dev. Med. Child Neurol.*, **52**, 868–872.
55. Allen, A.S., Berkovic, S.F., Cossette, P., Delanty, N., Dlugos, D., Eichler, E.E., Epstein, M.P., Glauser, T., Goldstein, D.B., Han, Y. *et al.* (2013) De novo mutations in epileptic encephalopathies. *Nature*, **501**, 217–221.
56. Zenker, M. (2011) Clinical manifestations of mutations in RAS and related intracellular signal transduction factors. *Curr. Opin. Pediatr.*, **23**, 443–451.
57. Niemeyer, C.M., Kang, M.W., Shin, D.H., Furlan, I., Erlacher, M., Bunin, N.J., Bunda, S., Finklestein, J.Z., Sakamoto, K.M., Gorr, T.A. *et al.* (2010) Germline CBL mutations cause developmental abnormalities and predispose to juvenile myelomonocytic leukemia. *Nat. Genet.*, **42**, 794–800.
58. Perez, B., Mechinaud, F., Galambrun, C., Ben Romdhane, N., Isidor, B., Philip, N., Derain-Court, J., Cassinat, B., Lachenaud, J., Kaltenbach, S. *et al.* (2010) Germline mutations of the CBL gene define a new genetic syndrome with predisposition to juvenile myelomonocytic leukaemia. *J. Med. Genet.*, **47**, 686–691.
59. Martinelli, S., De Luca, A., Stellacci, E., Rossi, C., Checquolo, S., Lepri, F., Caputo, V., Silvano, M., Buscherini, F., Consoli, F. *et al.* (2010) Heterozygous germline mutations in the CBL tumor-suppressor gene cause a Noonan syndrome-like phenotype. *Am. J. Hum. Genet.*, **87**, 250–257.
60. Fossat, N., Jones, V., Garcia-Garcia, M.J. and Tam, P.P. (2012) Modulation of WNT signaling activity is key to the formation of the embryonic head. *Cell Cycle*, **11**, 26–32.
61. Bassuk, A.G., Wallace, R.H., Buhr, A., Buller, A.R., Afawi, Z., Shimojo, M., Miyata, S., Chen, S., Gonzalez-Alegre, P., Griesbach, H.L. *et al.* (2008) A homozygous mutation in human PRICKLE1 causes an autosomal-recessive progressive myoclonus epilepsy-ataxia syndrome. *Am. J. Hum. Genet.*, **83**, 572–581.
62. Howlett, I.C., Rusan, Z.M., Parker, L. and Tanouye, M.A. (2013) Drosophila as a Model for Intractable Epilepsy: Gilgamesh Suppresses Seizures in parabss1 Heterozygote Flies. *G3 (Bethesda)*, **3**, 1399–1407.
63. Chan, D.W., Chan, C.Y., Yam, J.W., Ching, Y.P. and Ng, I.O. (2006) Prickle-1 negatively regulates Wnt/beta-catenin pathway by promoting Dishevelled ubiquitination/degradation in liver cancer. *Gastroenterology*, **131**, 1218–1227.
64. Foo, J.N., Liu, J.J. and Tan, E.K. (2012) Whole-genome and whole-exome sequencing in neurological diseases. *Nat. Rev. Nephrol.*, **8**, 508–517.
65. Veltman, J.A. and Brunner, H.G. (2012) De novo mutations in human genetic disease. *Nat. Rev. Genet.*, **13**, 565–575.
66. Sikkema-Raddatz, B., Johansson, L.F., de Boer, E.N., Almomani, R., Boven, L.G., van den Berg, M.P., van Spaendonck-Zwarts, K.Y., van Tintelen, J.P., Sijmons, R.H., Jongbloed, J.D. *et al.* (2013) Targeted next-generation sequencing can replace Sanger sequencing in clinical diagnostics. *Hum. Mutat.*, **34**, 1035–1042.
67. Singh, N.A., Westenskow, P., Charlier, C., Pappas, C., Leslie, J., Dillon, J., Anderson, V.E., Sanguinetti, M.C. and Leppert, M.F. (2003) KCNQ2 and KCNQ3 potassium channel genes in benign familial neonatal convulsions: expansion of the functional and mutation spectrum. *Brain*, **126**, 2726–2737.
68. Berkovic, S.F., Heron, S.E., Giordano, L., Marini, C., Guerrini, R., Kaplan, R.E., Gambardella, A., Steinlein, O.K., Grinton, B.E., Dean, J.T. *et al.* (2004) Benign familial neonatal-infantile seizures: characterization of a new sodium channelopathy. *Ann. Neurol.*, **55**, 550–557.
69. Lunter, G. and Goodson, M. (2011) Stampy: a statistical algorithm for sensitive and fast mapping of Illumina sequence reads. *Genome Res.*, **21**, 936–939.
70. Pagnamenta, A.T., Lise, S., Harrison, V., Stewart, H., Jayawant, S., Quaghebeur, G., Deng, A.T., Murphy, V.E., Akha, E.S., Rimmer, A. *et al.* (2012) Exome sequencing can detect pathogenic mosaic mutations present at low allele frequencies. *J. Hum. Genet.*, **57**, 70–72.
71. Wang, K., Li, M. and Hakonarson, H. (2010) ANNOVAR: functional annotation of genetic variants from high-throughput sequencing data. *Nucleic Acids Res.*, **38**, e164.
72. Conrad, D.F., Keebler, J.E., DePristo, M.A., Lindsay, S.J., Zhang, Y., Casals, F., Idaghdour, Y., Hartl, C.L., Torroja, C., Garimella, K.V. *et al.* (2011) Variation in genome-wide mutation rates within and between human families. *Nat. Genet.*, **43**, 712–714.
73. Davydov, E.V., Goode, D.L., Sirota, M., Cooper, G.M., Sidow, A. and Batzoglou, S. (2010) Identifying a high fraction of the human genome to be under selective constraint using GERP++. *PLoS Comput. Biol.*, **6**, e1001025.
74. Pollard, K.S., Hubisz, M.J., Rosenbloom, K.R. and Siepel, A. (2010) Detection of nonneutral substitution rates on mammalian phylogenies. *Genome Res.*, **20**, 110–121.
75. Siepel, A., Bejerano, G., Pedersen, J.S., Hinrichs, A.S., Hou, M., Rosenbloom, K., Clawson, H., Spieth, J., Hillier, L.W., Richards, S. *et al.* (2005) Evolutionarily conserved elements in vertebrate, insect, worm, and yeast genomes. *Genome Res.*, **15**, 1034–1050.
76. Chen, W., Han, Y., Chen, Y. and Astumian, D. (1998) Electric field-induced functional reductions in the K+ channels mainly resulted from supramembrane potential-mediated electroconformational changes. *Biophys. J.*, **75**, 196–206.
77. Watanabe, R., Inoue, N., Westfall, B., Taron, C.H., Orlean, P., Takeda, J. and Kinoshita, T. (1998) The first step of glycosylphosphatidylinositol biosynthesis is mediated by a complex of PIG-A, PIG-H, PIG-C and GPI1. *EMBO J.*, **17**, 877–885.
78. Ashida, H., Hong, Y., Murakami, Y., Shishioh, N., Sugimoto, N., Kim, Y.U., Maeda, Y. and Kinoshita, T. (2005) Mammalian PIG-X and yeast Pbn1p are the essential components of glycosylphosphatidylinositol-mannosyltransferase I. *Mol. Biol. Cell.*, **16**, 1439–1448.
79. O'Roak, B.J., Vives, L., Fu, W., Egertson, J.D., Stanaway, I.B., Phelps, I.G., Carvill, G., Kumar, A., Lee, C., Ankenman, K. *et al.* (2012) Multiplex targeted sequencing identifies recurrently mutated genes in autism spectrum disorders. *Science*, **338**, 1619–1622.

PIGA mutations cause early-onset epileptic encephalopathies and distinctive features

Mitsuhiro Kato, MD, PhD*
Hirotomo Saitsu, MD, PhD*
Yoshiko Murakami, MD, PhD*
Kenjiro Kikuchi, MD
Shuei Watanabe, MD
Mizue Iai, MD
Kazushi Miya, MD
Ryuki Matsuura, MD
Rumiko Takayama, MD
Chihiro Ohba, MD
Mitsuko Nakashima, MD, PhD
Yoshinori Tsurusaki, PhD
Noriko Miyake, MD, PhD
Shin-ichiro Hamano, MD
Hitoshi Osaka, MD, PhD
Kiyoshi Hayasaka, MD, PhD
Taroh Kinoshita, PhD
Naomichi Matsumoto, MD, PhD

ABSTRACT

Objective: To investigate the clinical spectrum caused by mutations in *PIGA* at Xp22.2, which is involved in the biosynthesis of the glycosylphosphatidylinositol (GPI) anchor, among patients with early-onset epileptic encephalopathies (EOEEs).

Methods: Whole-exome sequencing was performed as a comprehensive genetic analysis for a cohort of 172 patients with EOEEs including early myoclonic encephalopathy, Ohtahara syndrome, and West syndrome, and *PIGA* mutations were carefully investigated.

Results: We identified 4 *PIGA* mutations in probands showing early myoclonic encephalopathy, West syndrome, or unclassified EOEE. Flow cytometry of blood granulocytes from patients demonstrated reduced expression of GPI-anchored proteins. Expression of GPI-anchored proteins in *PIGA*-deficient JY5 cells was only partially or hardly restored by transient expression of PIGA mutants with a weak TATA box promoter, indicating a variable loss of PIGA activity. The phenotypic consequences of *PIGA* mutations can be classified into 2 types, severe and less severe, which correlate with the degree of PIGA activity reduction caused by the mutations. Severe forms involved myoclonus and asymmetrical suppression bursts on EEG, multiple anomalies with a dysmorphic face, and delayed myelination with restricted diffusion patterns in specific areas. The less severe form presented with intellectual disability and treatable seizures without facial dysmorphism.

Conclusions: Our study confirmed that *PIGA* mutations are one genetic cause of EOEE, suggesting that GPI-anchor deficiencies may be an underlying cause of EOEE. ***Neurology*® 2014;82:1587–1596**

GLOSSARY

ADC = apparent diffusion coefficient; **cDNA** = complementary DNA; **DWI** = diffusion-weighted image; **EME** = early myoclonic encephalopathy; **EOEE** = early-onset epileptic encephalopathy; **GPI** = glycosylphosphatidylinositol; **GPI-AP** = glycosylphosphatidylinositol-anchored protein; **OS** = Ohtahara syndrome; **WES** = whole-exome sequencing.

Correspondence to Dr. Kato: mkato@med.id.yamagata-u.ac.jp or Dr. Saitsu: hsaitsu@yokohama-cu.ac.jp

Supplemental data at Neurology.org

Early-onset epileptic encephalopathies (EOEEs) present with developmental impairment and disastrous seizures starting in early infancy with a mode of age dependency. Ohtahara syndrome (OS) and early myoclonic encephalopathy (EME), both of which show a distinctive EEG finding called suppression-burst pattern, are neonatal EOEEs. Genetic approaches have revealed some of the genes that are mutated in EOEEs. For instance, *ARX*, *STXBP1*, *CASK*, *KCNQ2*, and *SCN2A* are mutated in OS,[1–5] while *ARX*, *CDKL5*, and *SPTAN1* mutations cause West syndrome or infantile spasms.[6–8]

Mutations in 8 genes (*PIGA*, *PIGM*, *PIGN*, *PIGV*, *PIGL*, *PIGO*, *PIGT*, and *PGAP2*) involved in the biosynthesis of the glycosylphosphatidylinositol (GPI) anchor, a glycolipid structure embedded in the plasma membrane that attaches to hundreds of cell-surface proteins, have been identified in patients with a variety of multiple congenital anomalies, intellectual disability, and epileptic seizures.[9–16] Somatic mutations of *PIGA* at Xp22.2, which is involved in

*These authors contributed equally to this work.

From the Department of Pediatrics (M.K., K.H.), Yamagata University Faculty of Medicine, Yamagata; Department of Human Genetics (H.S., C.O., M.N., Y.T., N. Miyake, N. Matsumoto), Yokohama City University Graduate School of Medicine, Yokohama; Department of Immunoregulation (Y.M., T.K.), Research Institute for Microbial Diseases, and WPI Immunology Frontier Research Center, Osaka University, Suita; Division of Neurology (K.K., R.M., S.-i.H.), Saitama Children's Medical Center, Saitama; Division of Neurology (S.W.), Miyagi Children's Hospital, Sendai; Division of Neurology (M.I., H.O.), Clinical Research Institute, Kanagawa Children's Medical Center, Yokohama; Department of Pediatrics (K.M.), Graduate School of Medicine and Pharmaceutical Sciences, University of Toyama; Department of Pediatrics (R.T.), Aomori Prefectural Central Hospital, Aomori; and Department of Pediatrics (H.O.), Jichi Medical School, Tochigi, Japan.

Go to Neurology.org for full disclosures. Funding information and disclosures deemed relevant by the authors, if any, are provided at the end of the article.

the first step of the GPI biosynthesis, are responsible for paroxysmal nocturnal hemoglobinuria, and its germline mutation, were recently identified in a family with multiple congenital anomalies, neonatal seizures, and a poor prognosis.[11] At least 2 of 3 patients in this family showed severe myoclonic seizures with suppression bursts on EEG, strongly suggesting EME. The known mutations in EME prompted us to investigate *PIGA* in the EOEE patient cohort including EME and OS. We identified *PIGA* mutations in 5 patients from 4 families with EOEEs and present the clinical phenotypes of the patients and functional effects of the mutations in this study.

METHODS Patients. A total of 172 patients with EOEEs (2 with EME, 50 with OS, 50 with West syndrome or infantile spasms, 7 with malignant migrating partial seizures in infancy, and 63 with unclassified epileptic encephalopathy with an age at onset of <1 year; 90 male and 82 female patients) were analyzed by whole-exome sequencing (WES), and *PIGA* mutations were carefully investigated using WES data.

Patients had been mainly enrolled in the Japanese collaborative study for EOEE since 2003. The diagnosis was made based on clinical features and characteristic EEG patterns. Patients with mutations in *STXBP1*, *ARX*, *KCNQ2*, *SCN1A*, *SCN2A*, *KCNT1*, *CDKL5*, *CASK*, or *MECP2*, which were detected by high-resolution melting analysis, target capture analysis, direct sequencing analysis, or WES, were excluded from the study.

Whole-exome sequencing. Patient and parental genomic DNA was obtained from peripheral blood leukocytes using standard methods. DNA was captured using the SureSelectXT Human All Exon Kit (v4 or v5; Agilent Technologies, Santa Clara, CA) and sequenced on an Illumina HiSeq2000 (Illumina, San Diego, CA) with 101–base pair paired-end reads. Image analysis and base calling were performed using sequence control software real-time analysis and CASAVA software v1.8 (Illumina). Exome data processing, variant calling, and variant annotation were performed as previously described.[17–19] All novel mutations in *PIGA* were verified using Sanger sequencing.

Fluorescence-activated cell sorting analysis. Surface expression of GPI-anchored proteins (GPI-APs) was determined by staining cells with Alexa 488–conjugated inactivated aerolysin (FLAER; Protox Biotech, Victoria, Canada) and appropriate primary antibodies, namely, mouse anti-CD59 (5H8), DAF (IA10), CD16 (3G8), CD24 (ML5), and CD48 (BJ40), followed by a phycoerythrin-conjugated anti-mouse immunoglobulin G antibody (3G8, ML5, BJ40, and secondary antibodies; BD Biosciences, Franklin Lakes, NJ). Cells were analyzed by flow cytometry (Cant II; BD Biosciences).

Functional analysis using *PIGA*-deficient B lymphoblastoid cells (JY5). FLAG-tagged human *PIGA* complementary DNA (cDNA) and mutant cDNAs, generated by site-directed mutagenesis, were subcloned into the pMEoriP vector, a strong promoter (SRα)-driven vector or pTAoriP, a weak TATA box promoter-driven vector. Plasmid DNA was transfected by electroporation into *PIGA*-deficient JY5 cells. Expression of GPI-APs was analyzed by fluorescence-activated cell sorting. PIGA protein levels in transfected cells were determined by Western blotting using an anti-FLAG antibody (M2; Sigma, St. Louis, MO).

Standard protocol approvals, registrations, and patient consents. The experimental protocols were approved by the institutional review boards for ethical issues of Yamagata University Faculty of Medicine, Yokohama City University School of Medicine, and Osaka University, Japan. Written informed consent was obtained from all individuals and/or their families in compliance with relevant Japanese regulations. Permission for publishing photographs was also obtained from the parents.

RESULTS Identification of *PIGA* mutations. No mutations were found in *SLC25A22*, which had been reported in a family of EME.[20] We identified 4 hemizygous *PIGA* mutations in 3 sporadic patients and 2 siblings with EOEE. One mutation (c.1234C>T [p.R412X]) had previously been reported,[11] while the other 3 were novel missense mutations (c.230G>T [p.R77L], c.616A>T [p.I206F], and c.355C>T [p.R119W]). DNA from the mother of patient 1 (p.R412X) was unavailable. Three missense mutations were maternally inherited. All mutations were absent from the 6,500 exomes of the National Heart, Lung, and Blood Institute exome project and our 573 in-house control exomes (281 male and 292 female patients). All 4 mutations occurred at evolutionarily conserved amino acids (figure 1A) and were predicted to be highly damaging to the protein structure by SIFT, PolyPhen-2, and MutationTaster (table e-1 on the *Neurology*® Web site at Neurology.org), which supported their pathogenicity.

Clinical features of patients with the *PIGA* mutation. The clinical information of individuals with a *PIGA* mutation is summarized in table 1, and their facial appearances and representative brain images are shown in figures 1 and 2, respectively. EEG findings (figure e-1) and detailed case reports (appendix e-1) are available in supplemental data. Two patients were associated with polyhydramnios. Birth weight and length were normal in 3 patients (patients 2, 3, and 5) who were born at term, but the other 2 who were born at preterm showed higher (patient 1) or lower (patient 4) birth weights than normal. Three patients with the severe phenotype (patients 1, 2, and 5) showed facial dysmorphisms (figure 1, B and C), including a depressed nasal bridge, short anteverted nose, downturned corners of the mouth, and high arched palate. Patient 1 also showed bilateral vesicoureteral reflux of the most severe grade V. In addition, brain MRI demonstrated a thin corpus callosum and delayed myelination in these patients. Of interest, abnormally high signals on diffusion-weighted images (DWIs) and low signals on the apparent diffusion coefficient (ADC) map at the brainstem, basal ganglia, thalamus, and deep white matter were found in patients 1, 2, and 5 (figure 2, A–D and M–Q). By

Figure 1 *PIGA* mutations in patients with epileptic encephalopathy and dysmorphic features

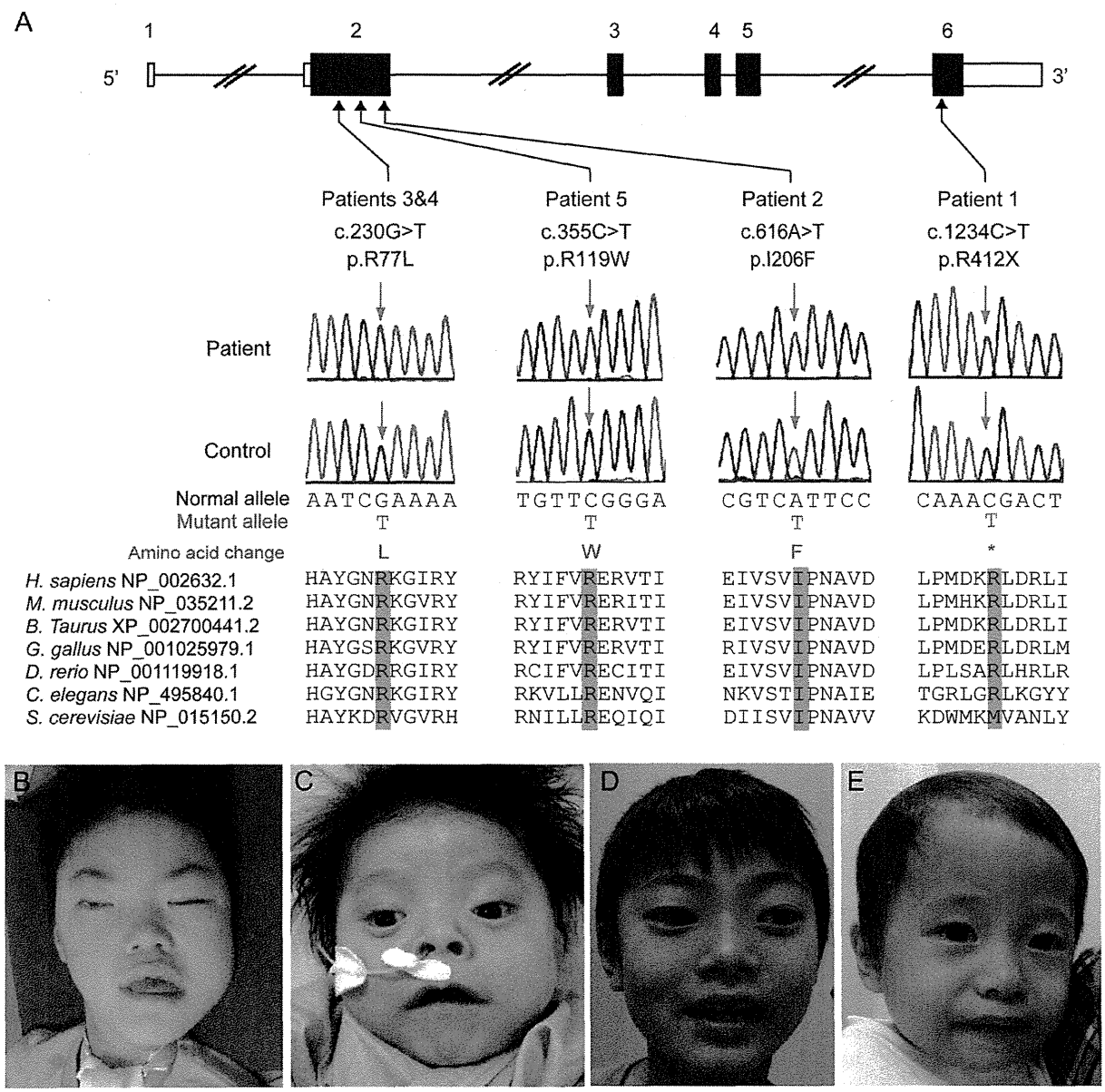

(A) Schematic presentation of *PIGA* genomic structure. Mutations are indicated based on the transcript variant 1 (GenBank accession number, NM_002641.3). Untranslated regions and coding regions are shown as white and black rectangles, respectively. All mutations occurred at evolutionarily conserved amino acids. Orthologous sequences were aligned using the CLUSTALW Web site. (B–E) Facial appearance of patients 2, 3, 4, and 5. Both patients 2 (B) and 5 (C) show distinct facial features, such as upslanting palpebral fissures, depressed nasal bridge, short anteverted nose, triangular mouth with downturned corners, and high arched palate, compared with patients 3 (D) and 4 (E) with no dysmorphic facial features.

contrast, 2 brothers with a less severe phenotype (patients 3 and 4) showed neither dysmorphic signs nor abnormalities in brain MRI (figure 2, E–L).

The first seizures started between 1 and 7 months of age, and tonic or myoclonic seizures occurred in all patients. Seizures of patients 1, 2, and 5 were refractory to antiepileptic medications, but topiramate was effective for the seizures of patient 3. The initial EEG showed a suppression burst in patient 1; patients 2 and 5 first demonstrated hypsarrhythmia, followed by a symmetrical or asymmetrical suppression burst later (figure e-1). Serum alkaline phosphatase levels were elevated in patients 2 and 5. No patients showed anemia or hemoglobinuria. All patients showed profound intellectual disability, and patients 1, 2, and 5 were bedridden with severe motor disturbance.

Flow cytometry. We analyzed the surface expression of various GPI-APs on patient granulocytes using flow

Table 1 Clinical summary of patients with a *PIGA* mutation

	Patients						
	IV-2	IV-4	1	2	3	4	5
Familial or sporadic	Familial or sporadic	Familial (brother)	Sporadic	Sporadic	Familial (proband)	Familial (brother)	Sporadic
Mutation	c.1234C>T (p.R412X)	c.1234C>T (p.R412X)	c.1234C>T (p.R412X)	c.616A>T (p.I206F)	c.230G>T (p.R77L)	c.230G>T (p.R77L)	c.355C>T (p.R119W)
Current age	Died at 11 wk	Died at 10 wk	6 y	10 y	8 y	18 mo	15 mo
Sex	M	M	M	M	M	M	M
Clinical diagnosis			Ohtahara syndrome, early myoclonic encephalopathy, Schinzel-Giedion syndrome	West syndrome with hypomyelination	Early-onset epileptic encephalopathy	Early-onset epileptic encephalopathy	West syndrome
Polyhydramnios	–	+	+	–	–	–	+
Gestation, wk	Full term	35	33	40	38	36	39
Birth weight, g	3,540	3,500	2,857	3,566	2,715	1,896	3,468
Birth length, *cm*	53.5	48	42.0	50	50	ND	47
Birth head circumference, cm	37	35.5	33.2	ND	32.5	ND	33.5
Facial dysmorphism	+	+	+	+	–	–	+
Vesicoureteral reflux	+	ND	+	ND	–	–	ND
Joint contractures	+	+	+	+	–	–	–
Hypotonia	+	+	+	–	–	–	+
Hyperreflexia	+	+	ND	–	–	–	+
Seizure onset	Neonate	Neonate	1 mo	3 mo	7 mo	7 mo	3 mo
Seizure types	Myoclonic	Severe myoclonic	Tonic seizures followed by frequent myoclonus	Myoclonus or epileptic spasm-like movement	Tonic seizures, secondarily generalized seizures	Tonic or clonic	Myoclonic seizures, tonic spasms
EEG findings	Suppression burst	Suppression burst	Suppression burst at neonatal period	Hypsarrhythmia at 3 mo, periodic bursts of multifocal epileptic discharges similar to suppression-burst pattern at 10 y	Normal at 7 mo, irregular spike and slow wave and multifocal spikes at 2 and 5 y	Normal at 7 mo	Hypsarrhythmia at 3 mo, suppression burst at 5 mo
Seizure prognosis	Intractable	Intractable	Intractable	Intractable	Seizure-free at 3 y with TPM	Seizure-free at 15 mo	Intractable
Development	Early death	Early death	Hypotonic quadriplegia, profound intellectual disability	Spastic quadriplegia, profound intellectual disability	Profound intellectual disability with autism, but no motor disturbance	Moderate intellectual disability, but no motor disturbance	Hypotonic quadriplegia, profound intellectual disability
Thin corpus callosum	+	+	+	+	–	–	+ (at 9 mo)
White matter immaturity	+	+	+	+	–	–	+ (at 9 mo)
Restricted diffusion pattern	ND	ND	+	+	–	–	+
Elevated serum alkaline phosphatase	ND	+	ND	+	–	–	+

Abbreviations: ND = not determined; TPM = topiramate.

Figure 2 Brain MRIs of patients with *PIGA* mutations

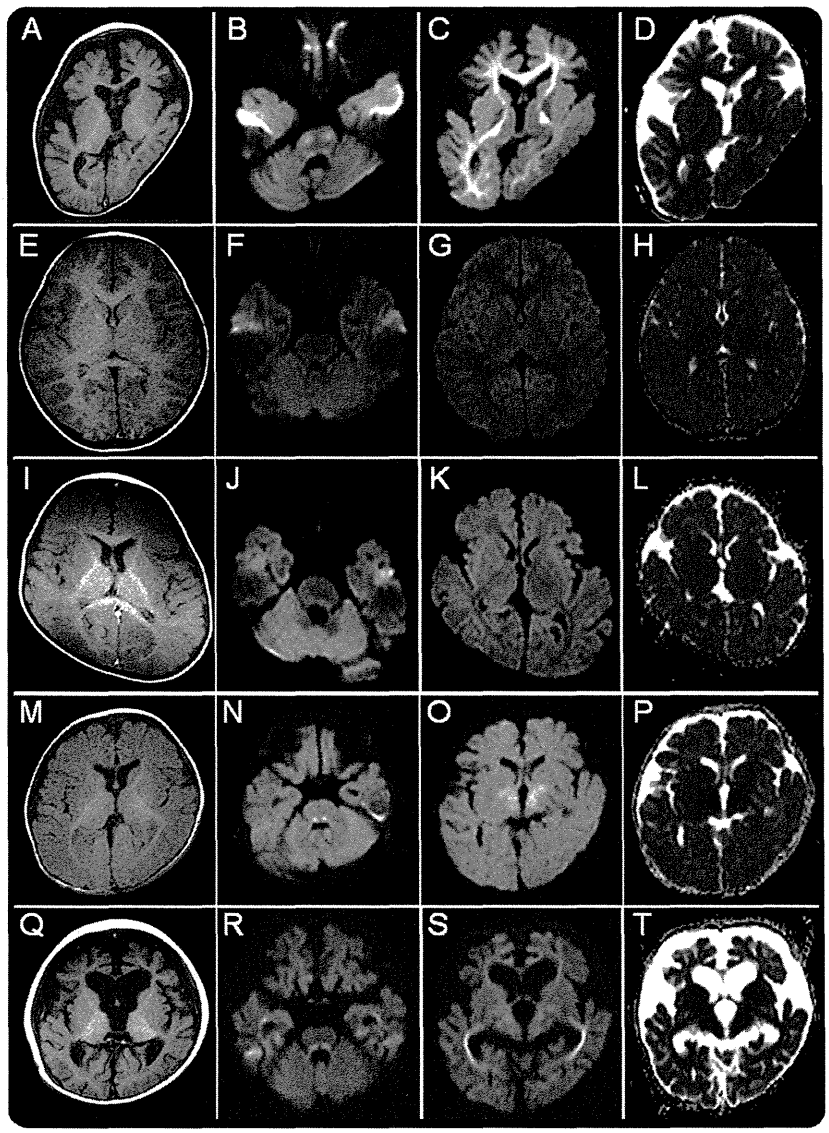

MRIs of patient 2 at 6 months (A) and 7 years (B–D), patient 3 at 3 years (E–H), patient 4 at 7 months (I–L), and patient 5 at 3 months (M–P) and 9 months (Q–T) of age. Left panels (A, E, I, M, Q) show axial T1-weighted images, the 2 middle panels (B, C, F, G, J, K, N, O, R, S) show axial diffusion-weighted images (DWIs), and right panels (D, H, L, P, T) show apparent diffusion coefficient (ADC) maps. Patient 2 and patient 5 at 9 months show cortical atrophy and enlarged ventricles. Note the high signals on DWI in the pontine tegmentum and deep white matter, particularly the optic radiation, of patients 2 and 5 in accordance with their age. The ADC map demonstrated decreased ADC within the same lesion. Patients 3 and 4 show normal images.

cytometry (figure 3). In all 5 patients, the surface expression of CD16 was severely decreased (from 5% to 15% of normal levels). Patient 1, with the most severe clinical symptoms, had a tendency to show reduced expression of other GPI-APs, such as CD24 and FLAER (figure 4A). Because *PIGA* is an X-linked gene and one allele is inactivated during early embryogenesis in female patients, patient mothers would be functionally mosaic for GPI-AP expression. Granulocytes from the mother of patients 3 and 4 showed a significantly decreased expression of CD16 (figure e-2, upper panels), whereas those from the mother of patient 5 showed normal expression (figure e-2, lower panels). The mothers appeared to have no neurologic disorder, suggesting that GPI-sufficient cells may preferentially proliferate in the brain during early embryogenesis.

Functional analysis. *PIGA* cDNAs bearing patient mutations were functionally analyzed by transfecting them into *PIGA*-deficient B lymphoblastoid cells (JY5) and measuring the surface expression of GPI-APs.

Figure 3 Flow cytometry of granulocytes

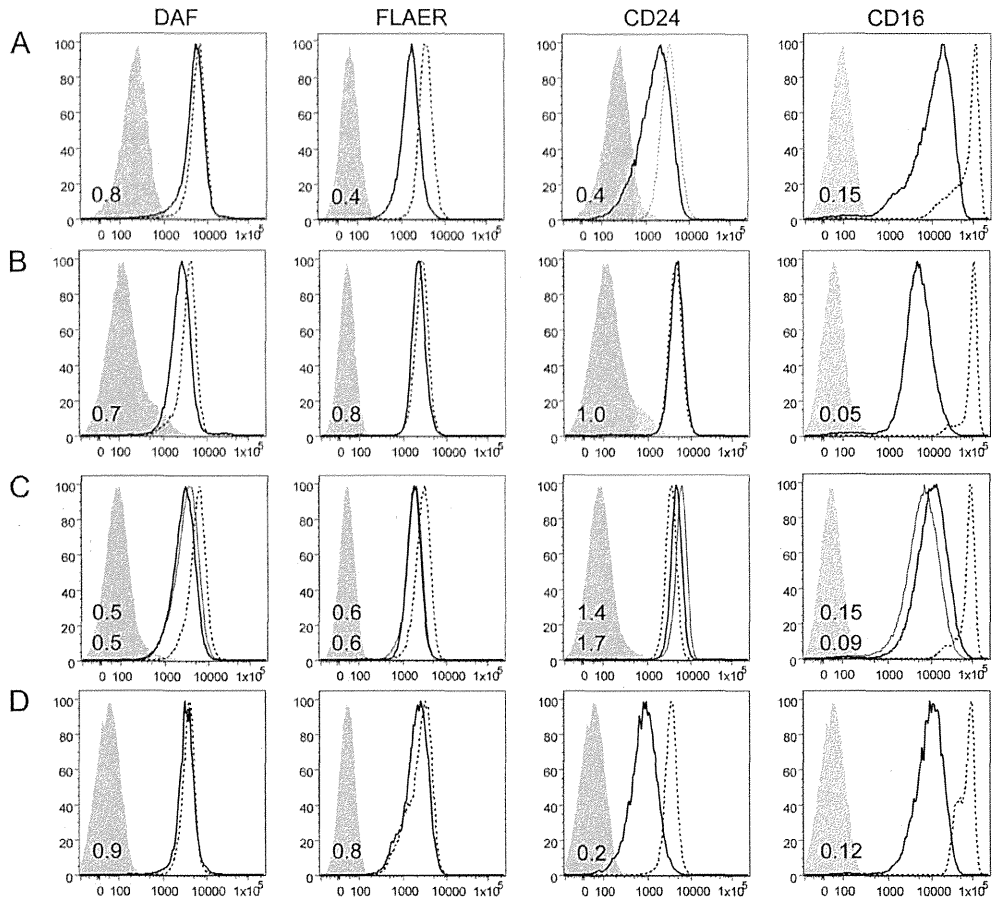

Flow cytometry of patient 1 (R412X) (A), patient 2 (I206F) (B), patients 3 and 4 (2 brothers, R77L) (C), and patient 5 (R119W) (D). In all families, the surface expression of various glycosylphosphatidylinositol-anchored proteins on patient granulocytes (solid lines; patients 3 and 4 are shown in C as thin and thick lines, respectively) was severely decreased compared with the normal control (dotted lines). Light shadows represent isotype controls. Mean fluorescent intensities of each sample against a normal control are shown in each panel (upper, patient 4; lower, patient 3 in C).

When strong promoter (SRα)-driven constructs were used, R412X mutant cDNA completely restored the surface expression of CD59, DAF, and CD48, whereas R412 truncated cDNA had no activity (figure 4A), suggesting that a small amount of full-length PIGA protein was generated by readthrough of a stop codon. When weak promoter-driven constructs (pTA) were used instead, R412X cDNA could not restore the surface expression of GPI-APs, whereas it was completely restored by wild-type cDNA (figure 4B). Similarly, the strong promoter (SRα)-driven I206F and R77L mutant PIGAs completely restored the surface expression of GPI-APs, whereas the weak promoter-driven mutant constructs only partially restored this (figure 4, C–F). Levels of expressed mutant PIGA proteins were similar to or even higher than wild-type levels (figure e-3). A faint band representing full-length PIGA protein harboring R412X could be detected (figure e-3, lane 4), which was consistent with the functional analysis. From these results, we concluded that these mutations affect the PIGA activity leading to inherited GPI deficiency.

DISCUSSION We have identified 4 *PIGA* mutations in 172 probands from a variety of EOEE-affected families, such as EME (n = 1), West syndrome (n = 2), and unclassified EOEE in a sibling. Myoclonus and suppression burst on EEG were recognized in 2 patients with West syndrome and the patient with EME in our cohort, as well as the previously reported family.[11] Indeed, myoclonus and suppression burst on EEG appear to be characteristic features for patients with a *PIGA* mutation.

Other clinical features such as polyhydramnios, facial dysmorphism, joint contractures, hypotonia, and severe developmental delay are recurrently seen in patients with *PIGA* mutations. A previous report of 3 patients with the same nonsense mutation,

Figure 4 Functional analysis of the mutant PIGA

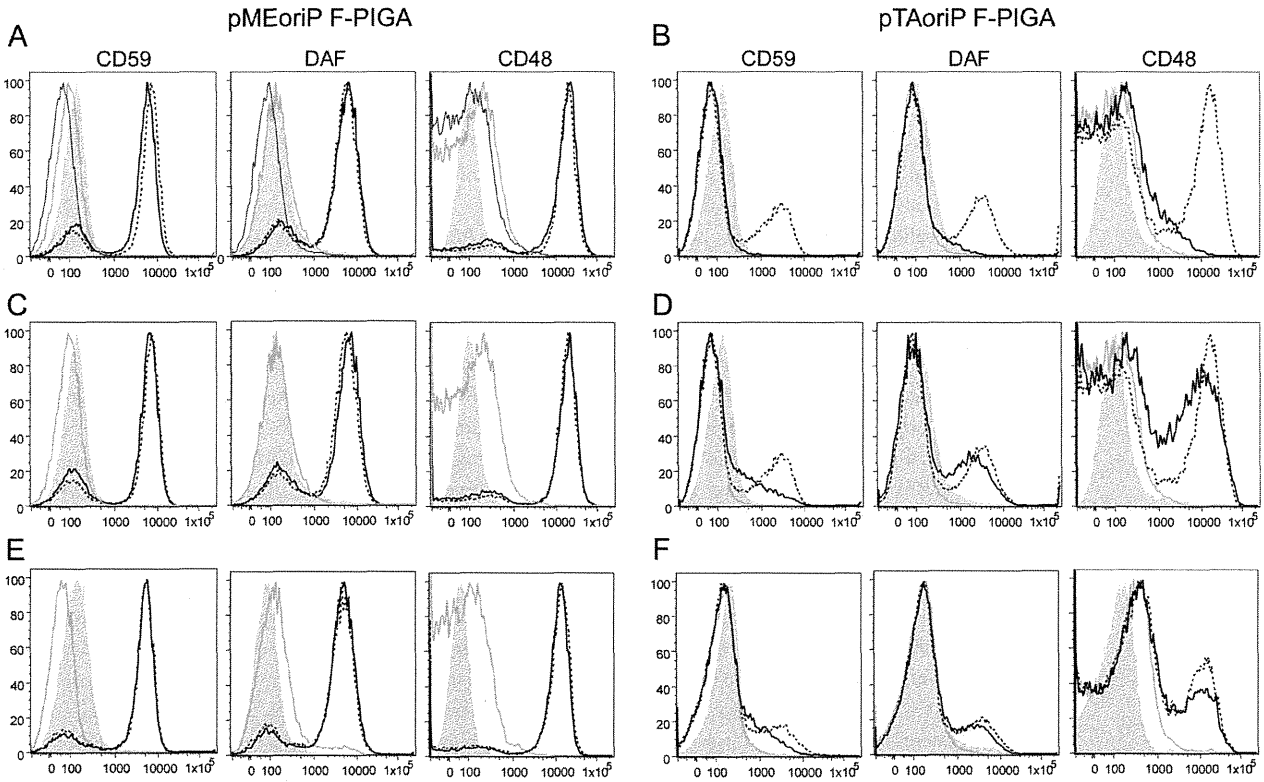

JY5 cells were transiently transfected with pMEoriP (strong SRα promoter-driven, Epstein-Barr [EB] virus origin-containing vector) (panels A, C, and E) or pTAoriP F-PIGA (weak TATA box promoter-driven, EB virus origin-containing vector) (panels B, D, and F) bearing various FLAG-tagged PIGA complementary DNAs. Restoration of the surface expression of CD59, DAF, and CD48 was assessed 2 days later by flow cytometry. Dotted lines represent wild-type PIGA, thick lines represent mutant PIGA, thin lines represent truncated PIGA, and shadows represent isotype controls. (A) Strong promoter-driven R412X PIGA (thick lines) completely rescued the expression of glycosylphosphatidylinositol-anchored proteins (GPI-APs) similar to wild-type PIGA (dotted lines), whereas R412-truncated PIGA (thin lines) had no activity. (B) Weak promoter-driven R412X PIGA (thick lines) did not rescue the surface expression of GPI-APs, whereas wild-type PIGA (dotted lines) did. (C) Strong promoter-driven I206F PIGA (thick lines) completely rescued the expression of GPI-APs similar to wild-type PIGA (dotted lines). (D) Weak promoter-driven I206F PIGA (thick lines) did not rescue the surface expression of GPI-APs, whereas wild-type PIGA (dotted lines) did. (E) Strong promoter-driven R77L PIGA (thick lines) completely rescued the expression of GPI-APs similar to wild-type PIGA (dotted lines). (F) Weak promoter-driven R77L PIGA (thick lines) did not rescue the surface expression of CD59, whereas wild-type PIGA (dotted lines) did.

R412X,[11] as patient 1 in our cohort showed similar or more severe clinical features, such as a large occipitofrontal circumference at birth, early-onset intractable seizures, and severe respiratory failure leading to early death or mechanical ventilation. Complete disruption of the *PIGA* gene results in early embryonic lethality in male mice, while heterozygous female mice have late embryonic lethality, insufficient closure of the neural tube, and a cleft palate.[21] In the present study, a reduced but definite expression of GPI-APs in the granulocytes of patients with R412X and a complete restoration of GPI-AP surface expression by the transfection of R412X mutant cDNA under the control of a strong promoter suggest that small amounts of full-length PIGA protein were generated by the read-through of a stop codon because the cDNA truncated at R412 showed no activity.

The siblings with the *PIGA* p.R77L mutation demonstrated milder clinical symptoms compared with patients with other *PIGA* mutations. They showed neither dysmorphisms nor severe motor disturbance, the onset of their seizures was relatively late, and the findings of their initial EEG and brain MRI were normal. Flow cytometry only revealed a decreased expression of CD16, which contrasts with the more severe phenotype of patient 1 and associated decreased levels of CD16, FLAER, and CD24. According to the functional study using *PIGA*-deficient B lymphoblasts transfected with a weak promoter-driven mutant *PIGA*, the activity of the R77L mutant was higher than that of other mutants. Thus, the phenotype severity appears to correlate with genotype and the residual functional activity of the PIGA protein.

Patients 2 and 5 showed peculiarly high signals on DWI at the specific areas of the brainstem, basal ganglia, thalamus, and deep white matter, particularly the optic radiation as previously reported in patient 1.[22] Although delayed myelination and the volume loss of

white matter including a thin corpus callosum, mild brain atrophy, and mild cerebellar hypoplasia are frequently seen in patients with mutations in other genes involved in the biosynthesis of the GPI anchor, such as *PIGN*, *PGAP2*, *DPM1*, and *DPM2*,[10,15,23,24] high signals on DWI have never been reported. In addition, the ADC map showed adversely low or decreased signals, suggesting restricted water diffusion. This pattern (a high DWI signal and low ADC values) can be seen in patients with specific metabolic disorders, such as nonketotic hyperglycinemia, phenylketonuria, maple syrup urine disease, Leigh encephalopathy, infantile neuroaxonal dystrophy, Wilson disease, metachromatic leukodystrophy, and Canavan disease.[25] Indeed, metabolic disorders, particularly nonketotic hyperglycinemia, are strongly associated with EME, which is common in patients with *PIGA* mutations. A brain MRI of a patient in early infancy with a recently reported *PIGO* deficiency also showed hypomyelination and abnormally high signals in T2-weighted images from the bilateral basal ganglia to the brainstem.[26] While the pathologic mechanism for restricted diffusion patterns in specific areas is unknown, this finding may be useful to screen patients with a GPI deficiency.

Patients with the severe type of *PIGA* mutation showed both an asymmetrical and symmetrical pattern of suppression burst on EEG in this study. The suppression burst pattern is characteristic for 2 types of EOEE, OS and EME, and most patients of both disorders show a symmetrical pattern. The asymmetrical pattern has been reported in patients with agenesis of the corpus callosum such as Aicardi syndrome,[27] and *KCNQ2* mutations.[4] All 3 patients with the asymmetrical suppression burst in the present study also showed white matter immaturity with a thin corpus callosum and abnormally high signals in deep white matter on DWI. These data indicate a disturbed connectivity of the bilateral hemisphere in patients with *PIGA* mutations. The adverse advancement of the EEG findings from hypsarrhythmia to suppression burst in our cases, which is usually observed in neonates, might reflect the retrogression of brain function, which is also seen in the progression of brain atrophy.

Patient 1 showed severe hydronephrosis caused by the vesicoureteral reflux and hepatoblastoma, so a diagnosis of Schinzel-Giedion syndrome was made. This is an autosomal dominant disorder characterized by severe developmental delay, distinctive facial features with a prominent forehead, midface retraction, short, upturned nose, and either hydronephrosis or typical skeletal malformations, such as sclerotic skull base, wide occipital synchondrosis, increased cortical density or thickness, and broad ribs.[28] *SETBP1* mutations have been reported in patients with Schinzel-Giedion syndrome[29] but were not identified in our patient. Because of the phenotypic similarities between patients with *PIGA* mutation and those with Schinzel-Giedion syndrome, we suggest that patients with Schinzel-Giedion syndrome with no *SETBP1* mutations should undergo genetic analysis of their *PIGA* gene or other genes involved in the biosynthesis of the GPI anchor.

Patients with mutations in *PIGL*, *PIGM*, *PIGN*, *PIGO*, *PIGT*, *DPM2*, and *MPDU1* often die in early childhood.[9,12,14–16,23,30] While pneumonia is the main cause of death in these patients, intractable seizures, which rigorously worsen the prognosis of life expectancy and cognitive function, frequently occur. It is of interest that the targeted agents butyrate and pyridoxine were reported to be effective for seizure treatment in patients with *PIGM* or *PIGO* mutation, respectively.[26,31] However, patient 5 in this study did not respond to pyridoxine. The study of more patients will facilitate the establishment of personalized treatment methods for patients with GPI deficiencies.

Our study demonstrated that mutations in *PIGA* are causative for a variety of EOEEs, particularly for patients with myoclonus and asymmetrical suppression burst on EEG. Multiple anomalies with facial dysmorphism resembling Schinzel-Giedion syndrome, delayed myelination with restricted diffusion patterns at the brainstem, and deep white matter are key findings in a severe form in patients with *PIGA* mutations. Nevertheless, a wide range of clinical phenotypes of *PIGA* mutations should be kept in mind, including the less severe forms involving intellectual disability and treatable seizures without facial dysmorphism.

AUTHOR CONTRIBUTIONS

Mitsuhiro Kato: study concept and design, analysis of the clinical data, interpretation of the data, and drafting/revising of the manuscript. Hirotomo Saitsu: study concept and design, analysis of the genetic data, interpretation of the data, and drafting/revising of the manuscript. Yoshiko Murakami: study concept and design, analysis of the biological data, interpretation of the data, and drafting/revising of the manuscript. Kenjiro Kikuchi, Shuei Watanabe, Mizue Iai, Kazushi Miya, Ryuki Matsuura, and Rumiko Takayama: analysis of the clinical data and sample collection. Chihiro Ohba, Mitsuko Nakashima, Yoshinori Tsurusaki, and Noriko Miyake: analysis of the genetic data. Shin-ichiro Hamano and Hitoshi Osaka: analysis of the clinical data and sample collection. Kiyoshi Hayasaka: analysis of the clinical data and revising of the manuscript. Taroh Kinoshita: analysis of the biological data, interpretation of the data, and drafting/revising of the manuscript. Naomichi Matsumoto: study concept and design, analysis of the genetic data, interpretation of the data, and drafting/revising of the manuscript.

ACKNOWLEDGMENT

The authors are grateful to the patients and their families for their participation in this study. The authors thank Keiko Tanaka, Kana Miyanagi, Nobuko Watanabe, and Kiyomi Masuko for their technical assistance.

STUDY FUNDING

This study was supported by the Ministry of Health, Labour and Welfare of Japan (25140101, 24133701,11103577, 11103340, 10103235), a Grant-in-Aid for Scientific Research (A), (B), and (C) from the Japan

Society for the Promotion of Science (A: 24249019, B: 25293085 25293235, C: 24591500, 23590363), the Takeda Science Foundation, the fund for Creation of Innovation Centers for Advanced Interdisciplinary Research Areas Program in the Project for Developing Innovation Systems, the Strategic Research Program for Brain Sciences (11105137), and a Grant-in-Aid for Scientific Research on Innovative Areas (transcription cycle, exploring molecular basis for brain diseases based on personal genomics) from the Ministry of Education, Culture, Sports, Science and Technology of Japan (12024421, 25129705).

DISCLOSURE

M. Kato is funded by research grants from the Ministry of Health, Labour and Welfare of Japan, and a Grant-in-Aid for Scientific Research (C) from the Japan Society for the Promotion of Science. H. Saitsu is funded by a Grant-in-Aid for Scientific Research (B) from the Japan Society for the Promotion of Science, and the Takeda Science Foundation. Y. Murakami is funded by a Grant-in-Aid for Scientific Research (C) from the Japan Society for the Promotion of Science, the Takeda Science Foundation, a Grant-in-Aid for Scientific Research on Innovative Areas (exploring molecular basis for brain diseases based on personal genomics) from the Ministry of Education, Culture, Sports, Science and Technology of Japan. K. Kikuchi, S. Watanabe, M. Iai, K. Miya, R. Matsuura, R. Takayama, C. Ohba, M. Nakashima, and Y. Tsurusaki report no disclosures relevant to the manuscript. N. Miyake is funded by research grants from the Ministry of Health, Labour and Welfare of Japan, a Grant-in-Aid for Scientific Research (B) from the Japan Society for the Promotion of Science, and the Takeda Science Foundation. S. Hamano, H. Osaka, and K. Hayasaka report no disclosures relevant to the manuscript. T. Kinoshita is supported by a Grant-in-Aid for Scientific Research (A) from the Japan Society for the Promotion of Science. N. Matsumoto is supported by grants from the Ministry of Health, Labour and Welfare of Japan, a Grant-in-Aid for Scientific Research (A) from the Japan Society for the Promotion of Science, the Takeda Science Foundation, the fund for Creation of Innovation Centers for Advanced Interdisciplinary Research Areas Program in the Project for Developing Innovation Systems, the Strategic Research Program for Brain Sciences, a Grant-in-Aid for Scientific Research on Innovative Areas (transcription cycle) from the Ministry of Education, Culture, Sports, Science and Technology of Japan. Go to Neurology.org for full disclosures.

Received November 7, 2013. Accepted in final form February 7, 2014.

REFERENCES

1. Kato M, Saitoh S, Kamei A, et al. A longer polyalanine expansion mutation in the *ARX* gene causes early infantile epileptic encephalopathy with suppression-burst pattern (Ohtahara syndrome). Am J Hum Genet 2007;81:361–366.
2. Saitsu H, Kato M, Mizuguchi T, et al. De novo mutations in the gene encoding STXBP1 (MUNC18-1) cause early infantile epileptic encephalopathy. Nat Genet 2008;40: 782–788.
3. Saitsu H, Kato M, Osaka H, et al. *CASK* aberrations in male patients with Ohtahara syndrome and cerebellar hypoplasia. Epilepsia 2012;53:1441–1449.
4. Kato M, Yamagata T, Kubota M, et al. Clinical spectrum of early onset epileptic encephalopathies caused by *KCNQ2* mutation. Epilepsia 2013;54:1282–1287.
5. Nakamura K, Kato M, Osaka H, et al. Clinical spectrum of *SCN2A* mutations expanding to Ohtahara syndrome. Neurology 2013;81:992–998.
6. Kato M. A new paradigm for West syndrome based on molecular and cell biology. Epilepsy Res 2006;70(suppl 1): S87–S95.
7. Saitsu H, Tohyama J, Kumada T, et al. Dominant-negative mutations in alpha-II spectrin cause West syndrome with severe cerebral hypomyelination, spastic quadriplegia, and developmental delay. Am J Hum Genet 2010;86:881–891.
8. Kurian MA, Meyer E, Vassallo G, et al. Phospholipase C beta 1 deficiency is associated with early-onset epileptic encephalopathy. Brain 2010;133:2964–2970.
9. Almeida AM, Murakami Y, Layton DM, et al. Hypomorphic promoter mutation in *PIGM* causes inherited glycosylphosphatidylinositol deficiency. Nat Med 2006;12: 846–851.
10. Hansen L, Tawamie H, Murakami Y, et al. Hypomorphic mutations in *PGAP2*, encoding a GPI-anchor-remodeling protein, cause autosomal-recessive intellectual disability. Am J Hum Genet 2013;92:575–583.
11. Johnston JJ, Gropman AL, Sapp JC, et al. The phenotype of a germline mutation in *PIGA*: the gene somatically mutated in paroxysmal nocturnal hemoglobinuria. Am J Hum Genet 2012;90:295–300.
12. Krawitz PM, Murakami Y, Hecht J, et al. Mutations in *PIGO*, a member of the GPI-anchor-synthesis pathway, cause hyperphosphatasia with mental retardation. Am J Hum Genet 2012;91:146–151.
13. Krawitz PM, Schweiger MR, Rodelsperger C, et al. Identity-by-descent filtering of exome sequence data identifies *PIGV* mutations in hyperphosphatasia mental retardation syndrome. Nat Genet 2010;42:827–829.
14. Kvarnung M, Nilsson D, Lindstrand A, et al. A novel intellectual disability syndrome caused by GPI anchor deficiency due to homozygous mutations in *PIGT*. J Med Genet 2013;50:521–528.
15. Maydan G, Noyman I, Har-Zahav A, et al. Multiple congenital anomalies-hypotonia-seizures syndrome is caused by a mutation in *PIGN*. J Med Genet 2011;48: 383–389.
16. Ng BG, Hackmann K, Jones MA, et al. Mutations in the glycosylphosphatidylinositol gene *PIGL* cause CHIME syndrome. Am J Hum Genet 2012;90:685–688.
17. DePristo MA, Banks E, Poplin R, et al. A framework for variation discovery and genotyping using next-generation DNA sequencing data. Nat Genet 2011; 43:491–498.
18. Saitsu H, Nishimura T, Muramatsu K, et al. De novo mutations in the autophagy gene *WDR45* cause static encephalopathy of childhood with neurodegeneration in adulthood. Nat Genet 2013;45:445–449.
19. Wang K, Li M, Hakonarson H. ANNOVAR: functional annotation of genetic variants from high-throughput sequencing data. Nucleic Acids Res 2010;38:e164.
20. Molinari F, Raas-Rothschild A, Rio M, et al. Impaired mitochondrial glutamate transport in autosomal recessive neonatal myoclonic epilepsy. Am J Hum Genet 2005;76: 334–339.
21. Nozaki M, Ohishi K, Yamada N, Kinoshita T, Nagy A, Takeda J. Developmental abnormalities of glycosylphosphatidylinositol-anchor-deficient embryos revealed by Cre/loxP system. Lab Invest 1999;79:293–299.
22. Watanabe S, Murayama A, Haginoya K, et al. Schinzel-Giedion syndrome: a further cause of early myoclonic encephalopathy and vacuolating myelinopathy. Brain Dev 2012;34:151–155.
23. Barone R, Aiello C, Race V, et al. DPM2-CDG: a muscular dystrophy-dystroglycanopathy syndrome with severe epilepsy. Ann Neurol 2012;72:550–558.
24. Yang AC, Ng BG, Moore SA, et al. Congenital disorder of glycosylation due to *DPM1* mutations presenting with dystroglycanopathy-type congenital muscular dystrophy. Mol Genet Metab 2013;110:345–351.

25. Sener RN. Diffusion magnetic resonance imaging patterns in metabolic and toxic brain disorders. Acta Radiol 2004; 45:561–570.
26. Kuki I, Takahashi Y, Okazaki S, et al. Vitamin B6-responsive epilepsy due to inherited GPI deficiency. Neurology 2013; 81:1467–1469.
27. Aicardi J. Aicardi syndrome. Brain Dev 2005;27: 164–171.
28. Lehman AM, McFadden D, Pugash D, Sangha K, Gibson WT, Patel MS. Schinzel-Giedion syndrome: report of splenopancreatic fusion and proposed diagnostic criteria. Am J Med Genet A 2008;146A: 1299–1306.
29. Hoischen A, van Bon BW, Gilissen C, et al. De novo mutations of *SETBP1* cause Schinzel-Giedion syndrome. Nat Genet 2010;42:483–485.
30. Kranz C, Denecke J, Lehrman MA, et al. A mutation in the human *MPDU1* gene causes congenital disorder of glycosylation type If (CDG-If). J Clin Invest 2001;108:1613–1619.
31. Almeida AM, Murakami Y, Baker A, et al. Targeted therapy for inherited GPI deficiency. N Engl J Med 2007;356: 1641–1647.

PLOS | GENETICS

Null Mutation in PGAP1 Impairing Gpi-Anchor Maturation in Patients with Intellectual Disability and Encephalopathy

Yoshiko Murakami[1]*, Hasan Tawamie[2], Yusuke Maeda[1], Christian Büttner[2], Rebecca Buchert[2], Farah Radwan[2], Stefanie Schaffer[3], Heinrich Sticht[4], Michael Aigner[3], André Reis[2], Taroh Kinoshita[1], Rami Abou Jamra[2]*

1 Research Institute for Microbial Diseases and WPI Immunology Frontier Research Center, Osaka University, Suita, Osaka, Japan, **2** Institute of Human Genetics, Friedrich-Alexander-Universität Erlangen-Nürnberg, Erlangen, Germany, **3** Department of Internal Medicine 5, Hematology and Oncology, University of Erlangen-Nürnberg, Erlangen, Germany, **4** Institute of Biochemistry, Friedrich-Alexander-Universität Erlangen-Nürnberg, Erlangen, Germany

Abstract

Many eukaryotic cell-surface proteins are anchored to the membrane via glycosylphosphatidylinositol (GPI). There are at least 26 genes involved in biosynthesis and remodeling of GPI anchors. Hypomorphic coding mutations in seven of these genes have been reported to cause decreased expression of GPI anchored proteins (GPI-APs) on the cell surface and to cause autosomal-recessive forms of intellectual disability (ARID). We performed homozygosity mapping and exome sequencing in a family with encephalopathy and non-specific ARID and identified a homozygous 3 bp deletion (p.Leu197del) in the GPI remodeling gene *PGAP1*. *PGAP1* was not described in association with a human phenotype before. PGAP1 is a deacylase that removes an acyl-chain from the inositol of GPI anchors in the endoplasmic reticulum immediately after attachment of GPI to proteins. In silico prediction and molecular modeling strongly suggested a pathogenic effect of the identified deletion. The expression levels of GPI-APs on B lymphoblastoid cells derived from an affected person were normal. However, when those cells were incubated with phosphatidylinositol-specific phospholipase C (PI-PLC), GPI-APs were cleaved and released from B lymphoblastoid cells from healthy individuals whereas GPI-APs on the cells from the affected person were totally resistant. Transfection with wild type *PGAP1* cDNA restored the PI-PLC sensitivity. These results indicate that GPI-APs were expressed with abnormal GPI structure due to a null mutation in the remodeling gene *PGAP1*. Our results add *PGAP1* to the growing list of GPI abnormalities and indicate that not only the cell surface expression levels of GPI-APs but also the fine structure of GPI-anchors is important for the normal neurological development.

Citation: Murakami Y, Tawamie H, Maeda Y, Büttner C, Buchert R, et al. (2014) Null Mutation in PGAP1 Impairing Gpi-Anchor Maturation in Patients with Intellectual Disability and Encephalopathy. PLoS Genet 10(5): e1004320. doi:10.1371/journal.pgen.1004320

Editor: Stefan Mundlos, Max Planck Institute for Molecular Genetics, Germany

Received October 24, 2013; **Accepted** March 7, 2014; **Published** May 1, 2014

Funding: This study was supported by the German Intellectual disability Network (MRNET) through a grant from the German Ministry of Research and Education to AR (01GS08160 and 01GR0804-4), by the Deutsche Forschungsgemeinschaft (DFG) through a grant to RAJ (AB393/2-1), by the Deutscher Akademischer Austauschdienst (DAAD) through a scholarship to HT, by Deutsche Forschungsgemeinschaft and Friedrich-Alexander-Universität Erlangen-Nürnberg (FAU) within the funding programe Open Access Publishing, by grants from the Ministry of Education, Culture, Sports, Science, and Technology of Japan (a Grant-in-Aid for Scientific Research C 23590363 and a Grant-in-Aid for Scientific Research on Innovative Areas, Exploring molecular basis for brain diseases based on personal genomics 25129705), and from the Takeda Science Foundation. The funders had no role in study design, data collection and analysis, decision to publish, or preparation of the manuscript.

Competing Interests: The authors have declared that no competing interests exist.

* E-mail: yoshiko@biken.osaka-u.ac.jp (YM); rami.aboujamra@uk-erlangen.de (RAJ)

Introduction

Many eukaryotic cell-surface proteins with various functions are anchored to the membrane via glycosylphosphatidylinositol (GPI) [1–3]. After biosynthesis in the endoplasmic reticulum (ER), GPI-anchors are transferred to the proteins by the GPI transamidase and the structure of the GPI-anchor is then remodeled, which is critical for sorting, regulating and trafficking of the GPI anchored proteins (GPI-APs) [3]. This remodeling starts in the ER by eliminating the acyl-chain linked to the inositol in the GPI-anchor by PGAP1 [4], then a side-chain of ethanolamine-phosphate on the second mannose of the GPI-anchor is removed by MPPE1 (PGAP5) [5]. GPI-APs are then transported from the ER to the plasma membrane through the Golgi apparatus, where further remodeling by PGAP3 and PGAP2 takes place [6,7]. Germline mutations in eight genes that are involved in the GPI-anchor biosynthesis and remodeling have been described (Table 1) [8–22]. The mutations in all of those, *PIGA*, *PIGL*, *PIGM*, *PIGV*, *PIGN*, *PIGO*, *PIGT* and *PGAP2*, are hypomorphic and lead to partially decreased cell surface expression of various GPI-APs, thus causing a wide phenotypic spectrum ranging from syndromic disorders with various malformations to non-specific forms of intellectual disability. The reported mutations in genes of early steps of the GPI-anchor synthesis such as *PIGA* (MIM 311770), *PIGL* (MIM 605947), and *PIGM* (MIM *610273), or in a gene involved in GPI transfer to proteins such as *PIGT* (MIM *610272) are supposed to result in a degradation of precursor non-GPI-anchored proteins by ER associated degradation, whereas mutations in genes that are involved in later steps of the pathway, such as *PIGV* (MIM *610274), *PIGO* (MIM *614730), and *PGAP2* (MIM *615187)

Author Summary

Glycosylphosphatidylinositols (GPI) are glycolipid anchors that anchor various proteins to the cell surface. At least 26 genes are involved in biosynthesis and modification of the GPI anchors. Recently, mutations in eight of those genes have been described. Although those mutations do not fully abolish the functions of encoded enzymes, they lead to a decreased expression of surface GPI-anchored proteins and to different forms of intellectual disability. Here we report a mutation in *PGAP1* that encodes a protein that modifies the GPI anchor. We found that the mutation leads to a full loss of PGAP1 enzyme activity, but that the patient cells still express normal levels of surface GPI-anchored proteins. However, the GPI anchors have an abnormal lipid structure that is resistant to cleavage by phosphatidylinositol-specific phospholipase C. Our results add *PGAP1* to the growing list of GPI abnormalities that cause intellectual disability and indicate that the fine structure of GPI-anchors is also important for a normal neurological development.

result in partial secretion of non-GPI-anchored proteins such as alkaline phosphatase (in case of *PIGV* or *PIGO* deficiency) [23] or of proteins bearing cleaved GPI-anchor (in case of *PGAP2* deficiency), and are therefore characterized by hyperphosphatasia. Here we report on the identification of a mutation in *PGAP1* that encodes the GPI inositol-deacylase [4]. This leads to a new type of GPI-anchor deficiency manifesting non-specific autosomal recessive intellectual disability (ARID), in which cell surface levels of GPI-APs are not affected whereas the structure of GPI moiety is abnormal.

Results

Clinical manifestations

We undertook clinical characterization, mapping [24] and exome sequencing in a large cohort of families with non-specific ARID. We identified the *PGAP1* mutation in the Syrian family MR079. The parents in family MR079 are the first-degree cousins and the family has one healthy girl and two affected children that carry the mutation in a homozygous status. The affected girl (III-2) was 4 years and 5 months old and the affected boy (III-3) was 2 years and 9 months old at the time of examination (Figure 1). Pregnancy, delivery, and birth parameters of both children were unremarkable. In the neonatal period, III-2 was hypotonic and III-3 was a floppy baby. Motor development was delayed; III-2 could sit at age of 18 months and at age of $4^{5/12}$ years first tried to walk independently. At age of $2^{9/12}$, III-3 could only roll from back to stomach and back. Both children did not finish potty training and were still partially fed with milk bottles. Both children have a developmental delay and severe intellectual disability with an estimated IQ below 35. III-2 could only babble a few syllables. While III-2 had major and absence epilepsy, III-3 did not yet have seizures. Sleeping patterns of both children were normal. They showed some stereotypic movements such as hitting on their own mouth and some washing movements of the hands. Both children seemed to see and hear properly, but specific tests could not be done. Brain CT scan of III-2 at age of one year revealed pronounced brain atrophy. At the time of examination, III-2 was 96 cm tall (25^{th} percentile) with a head circumference of 46 cm (2 cm below the 5^{th} percentile). III-3 was also of normal height and had a head circumference of 47 cm (1.5 cm below the 5^{th} percentile). Their parents had head circumferences of 52 and 53 cm, also in the lower percentiles. Both children have large ears and a flattened nasal root. G-banding, cytogenetic examination and genome wide copy number variants analyses were unremarkable. We did not have information on the levels of alkaline phosphatase and it was not possible to obtain blood probes retrospectively.

Exome sequencing revealed a homozygous mutation in *PGAP1*

Autozygosity mapping [24] in family MR079 led to the identification of six candidate regions of a total length of 64 Mb. Subsequently, exome sequencing using DNA from individual III-3 was performed as described in former studies [21,25] resulting in an average coverage of 53.28. 66% of the target sequences were covered with a depth of at least 20×, and 80.51% were covered with a depth of at least 5×. A total of 42,352 SNVs and 2,529 indels were identified. 342 SNVs and 64 indels were neither annotated, nor reported in 1000Genomes and Exome Variant Server, nor in in-house controls, and may affect the protein sequence (non-synonymous, splicing, or UTR). Of those, only two, in *PGAP1* and *SLC40A*, were located in a candidate region, conserved, and predicted to be pathogenic by *in silico* programs. To exclude further candidate mutations, we repeated the exome sequencing using DNAs of both affected siblings. We enriched the exome using a PCR based targeting method (Ion AmpliSeq Exome Kit) and sequenced on the Ion Proton. The average coverage of III-3 and III-2 was 149.6× and 94.6×, respectively. 91.1% and 85.0% of the target sequences were covered with a depth of at least 20×, 96.3% and 93.4% with a depth of at least 5×, respectively. A total of 49,455 and 47,693 SNVs as well as 3,343 and 3,167 indels were identified. When applying the above mentioned filtering steps, we were by both affected children once again left with the variants in *PGAP1* and *SLC40A*. Since mutations in *SLC40A* cause hemochromatosis of type 4 and have no effect on cognition (MIM 606069) [26,27], we focused on the variant in *PGAP1*, NM_024989.3:c.589_591delCTT, NP_079265.2:p.Leu197-del. Genotyping the variant in *PGAP1* in 372 healthy Syrian adults using Sanger sequencing revealed no further carriers. Taking the minor allele frequency of 0 in the Exome Sequencing Project (ESP) data set and in our control sample of 372 healthy Syrian individuals, it seems that the mutation has prevalence far less than 0.001.

Molecular modeling using the GeneSilico fold recognition metaserver [28] and Modeler9.9 [29] using the closest related hydrolase (PDB code: 3LP5) as template highlighted the detrimental effect of the deletion of leucine 197 on the structure of PGAP1. Leucine 197 is located in the central strand of a β-sheet and is oriented towards the hydrophobic core of the enzyme where it forms multiple stabilizing interactions with the adjacent helices (Figure 2A, B). Deletion of this amino acid would place Ile198 at the position originally occupied by Leu197 (Figure 2C). The Cβ-branched side-chain of isoleucine cannot be accommodated at this sequence position resulting in several clashes with adjacent amino acids (Leu184, Ile194) of the hydrophobic core (Figure 2C). This will disrupt the packing of the hydrophobic core and consequently of the entire β-sheet topology, thus leading to a loss of tertiary structure and enzymatic activity.

We then ran large scale homozygosity mapping using PLINK in our sample of over 100 consanguineous families [24] and over 600 sporadic cases of ID [30] and identified 7 index patients, 2 from consanguineous families with multiple affected children and 5 from outbreed families with single affected patients, that are homozygous at the *PGAP1*. Sequencing all seven individuals using Sanger did not reveal any mutations in *PGAP1*.

Table 1. Overview of identified mutations in the GPI synthesis pathway and the associated symptoms.

Gene (RefSeq)	Phenotypes	Families	Mutations	References
PIGA (NM_002641.3)	Multiple congenital anomalies involving cleft palate, neonatal seizures, central nervous system structural malformations, intellectual disability	3	homo[1] p.R412* homo p.Leu110del homo p.Pro93Leu	[9,10,11]
PIGL (NM_004278.3)	Coloboma, congenital heart disease, ichthyosiform dermatosis, intellectual disability, ear anomalies	5	comp het[2] p.Leu167Pro & p.Leu92Phefs*15 comp het p.Leu167Pro & p.Gln218* homo p.Leu167Pro comp het p.Leu167Pro & c.427-1G>A (Splice defect) comp het p.Leu167Pro & p.del17p12-p11.2	[19]
PIGM (NM_145167.2)	Portal and hepatic vein thrombosis in early childhood and seizures, no intellectual disability	2	promoter GC-BOX	[8]
PIGV (NM_017837.3)	Intellectual disability, characteristic face, seizures, brachytelephalangy, hyperphosphatasia,	14	homo p.Leu302Pro homo p.Ala341Glu comp het p.Ala341Glu & p.Leu59Arg comp het p.Ala341Glu & p.Cys18Tyr comp het p.Ala341Glu p.Arg469* comp het p.Ala341Glu & p.His385Pro homo p.Gly256Lys comp het p.Ala341Glu & p.Ala341Val comp het p.Ala341Glu & p.Cys156Tyr comp het p.Pro165Gln & p.Cys156Tyr	[13,14]
PIGN (NM_012327.5)	Multiple congenital anomalies, hypotonia, seizures, intellectual disability	2	homo p.Arg709Gln comp het p.Ser270Pro & c.963G>A (Splice defect)	[17,18]
PIGO (NM_032634.3)	Intellectual disability, recognizable facial characteristics, seizures, brachytelephalangy, hyperphosphatasia	4	comp het p.Leu957Phe & c.3069+5G>A(Splice defect) comp het p.Thr788Hisfs*5 & p.Leu957Phe comp het p. Arg119trp & p. Ala834fs*129 comp het p.Gln430* & p.Thr130Asn	[12,15,16]
PIGT (NM_015937)	Intellectual disability, hypotonia, characteristic facial features, seizures, and further skeletal, endocrine, and ophthalmologic findings, hypophosphatasia	1	homo p.Thr183Pro	[20]
PGAP1 (NM_024989.3)	Intellectual disability, major and absence epilepsy in 1 sibling, brain atrophy on CT scan	1	homo p.Leu197del	This study
PGAP2 (NM_001256240.1)	Severe intellectual disability, absence seizures, hyperphosphatasia	3	homo p.Tyr99Cys homo p.Arg77Pro comp het p.Arg16Trp & p.Thr160Ile	[21,22]

1: homozygous,
2: compound-heterozygous.
doi:10.1371/journal.pgen.1004320.t001

We then screened the exome variant server for functional variants in *PGAP1*. 149 variants are reported in this gene, of those 44 were coding or at splice sites. All of those are extremely rare (0.0077%–0.569%, i. e. 1–74 alleles out of ca. 13000 alleles). Based on the conservation of the variants and the prediction of *in silico* programs (Table S1), we roughly estimate that a maximum of 48 individuals may carry a mutation in *PGAP1* (carrier rate of 48/6500 = 0.0073) and that the prevalence of the disease would be about 13 per million. If we take more conservative *in silico* prediction numbers, the prevalence of the disease would be 7 per million inhabitants (Table S1). The two most frequent variants in the ESP data were p.Lys111Glu and p.Gln585Glu and were observed in a heterozygous form 15 and 74 times out of 12992 and 12932 alleles, respectively. Both sites are well conserved in the mammalian. Molecular modeling showed that the most common variant Gln585Glu is located outside of catalytic active domains and it was not possible to make a prediction for this variant. Lys111Glu is at the C terminus of a helix of the deacylase domain. The charging pattern of the helix is highly conserved so that we expect that the change from Lys to Glu would change the charge of the protein and destabilize the helix.

Flow cytometry of B-lymphoblastoid cell lines

To determine effects of p.Leu197del alteration on cellular GPI-APs, we investigated the surface expression of GPI-APs on B-lymphoblastoid cell lines (LCLs) derived from the homozygous

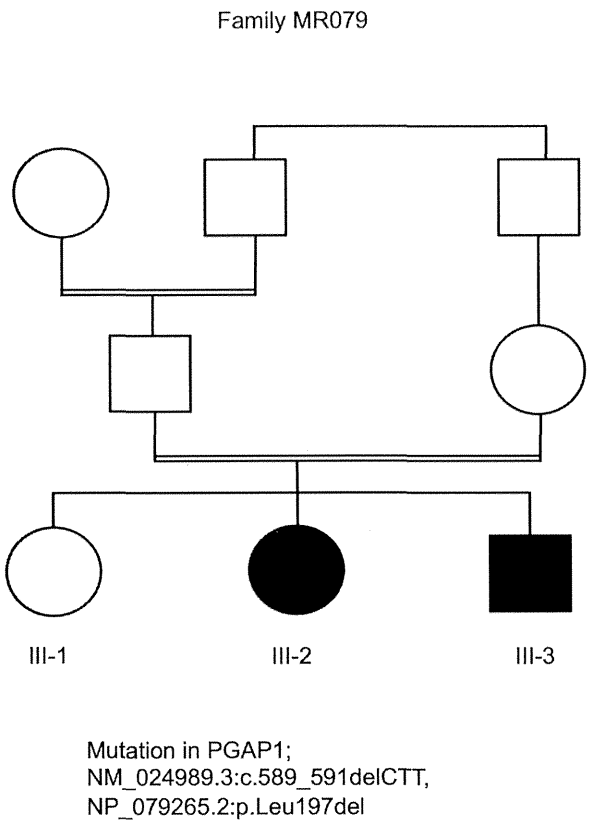

Figure 1. Pedigree of family MR079 and a PGAP1 mutation.
doi:10.1371/journal.pgen.1004320.g001

individual III-3 (−/−), 2 heterozygous parents (+/−), and the healthy sister (+/+) (Figure 3), as well as 6 healthy volunteers with a confirmed wild type genotype (data not shown). Using flow cytometry analysis, the respective surface expressions of CD59, CD55/DAF, and CD48 were quantified. Surface expression of these GPI-APs on LCLs from an affected person, other family members or healthy volunteers showed no significant difference, indicating that the *PGAP1* mutation did not affect the surface expression levels of various GPI-APs (Figure 3A, dotted lines). The surface expression of the GPI anchor itself was quantified using fluorochrome conjugated aerolysin (FLAER, Pinewood Scientific), a bacterial toxin that specifically binds GPI anchors, and did not show significant differences between the affected individual, the heterozygous individuals, and the controls (data not shown).

Altered GPI anchors are resistant to PI-PLC cleavage

We then investigated the expected structural abnormality of GPI-anchors by testing sensitivity of GPI-APs to phosphatidylinositol-specific phospholipase C (PI-PLC) [31]. The LCLs were incubated with 10 unit/ml of PI-PLC for 1.5 h at 37°C and the remaining surface GPI-APs were determined by flow cytometry. Of GPI-APs, 61% to 90% were removed from the surface of LCLs of the healthy sister with a homozygous wildtype (Figure 3A, solid line) and healthy control individuals (data not shown). In contrast, no significant or only slight reduction of the surface GPI-APs was seen with LCLs from the affected person (Figure 3A), indicating that almost all GPI-APs on the affected LCLs had abnormal GPI anchors resistant to PI-PLC [4]. This is a strong indication that the p.Leu197del mutation causes null or almost null activity of the PGAP1 enzyme. GPI-APs on LCLs from heterozygous parents were only partially sensitive to PI-PLC (Figure 3A), indicating that the p.Leu197del mutation causes haplo-insufficiency. These defective sensitivities of affected the person's and parents' GPI-APs to PI-PLC were fully restored by transfection of wild-type *PGAP1* cDNA (Figure 3B, solid lines).

Finally, the functional effect of the p.Leu197del mutation was tested in the *PGAP1* deficient Chinese hamster ovary (CHO) cell system [4]. GPI-APs expressed on the *PGAP1* deficient CHO cells are resistant to PI-PLC and the activity of *PGAP1* cDNA can be assessed by its ability to make PI-PLC-sensitive GPI-APs after transfection. CHO cells defective for *PGAP1* were transiently transfected with N-terminally-FLAG-tagged wild-type and p.Leu197del mutant human *PGAP1* cDNA in an expression vector with a strong SRα promoter, or an empty vector. Four days after transfection, each transfectant was treated with or without PI-PLC, and the surface expression of CD59, DAF and urokinase plasminogen activator receptor (uPAR) were assessed by flow cytometry. The wild-type *PGAP1* cDNA rescued PI-PLC sensitivity (Figure 4A, left panels). In contrast, the transfection of the mutant p.Leu197del cDNA did not increase the sensitivity to PI-PLC, thus indicating functional loss of the mutant *PGAP1* cDNA (Figure 4A, center panels). To determine PGAP1 protein levels, lysates were prepared two days after transfection, immunoprecipitated with anti-FLAG beads and analyzed by SDS-PAGE/Western blotting. The p.Leu197del mutant protein was not detected at all, indicating that the deletion of Leu197 caused an unstable protein (Figure 4B).

In order to evaluate other known variants in *PGAP1*, we screened the public database of ESP (see above). Of listed variants, we chose the two most frequent variants: rs142320636: c.331A>G (p.Lys111Glu) and rs62185645: c.1753C>G (p.Gln585Glu), and tested the functional effect of these mutations in the *PGAP1* deficient Chinese hamster ovary (CHO) cell system. Transfection of the mutant p.Lys111Glu cDNA did not increase the sensitivity to PI-PLC, indicating functional loss of the mutant *PGAP1* cDNA. Mutant p.Gln585Glu showed an activity comparable to the wild type PGAP1 (Figure S1). Thus, it is possible that homozygosity of p.Lys111Glu leads to ARID.

Discussion

Eight GPI deficiencies caused by hypomorphic mutations in the coding regions of GPI biosynthesis genes *PIGM*, *PIGA*, *PIGL*, *PIGV*, *PIGN*, *PIGO*, *PIGT*, and *PGAP2* have been reported. Except *PIGM*, all lead to a decreased surface expression of GPI-APs and result in intellectual disability, often associated with epilepsy, distinct facial characteristics, and further organ malformations [9–22]. We showed here that complete *PGAP1* deficiency did not affect the surface expression of GPI-APs but expressed structurally abnormal GPI-APs with the acylated inositol.

In previous works, we have reported that *Pgap1* knock-out mice had otocephaly, male infertility, growth retardation, and often died right after birth [32]. Also further two mutant mouse strains, *oto*^{xrqy} (*oto* for otocephaly) [33,34] and *beaker* [35] were reported to have disrupted *Pgap1*. Both mice strains showed developmental abnormalities of the forebrain; the recessive lethal *oto*^{xrqy} showed a truncation of the forbrain and the *breaker* mutant displayed a holoprosencephaly-like phenotype. Both Wnt signaling and Nodal signaling were reported to be affected in these mutant mice. These data emphasize the importance of *PGAP1* for vital functions and for brain development. It was also indicated that the *Pgap1* mutant mice phenotypes are dependent upon the genetic background

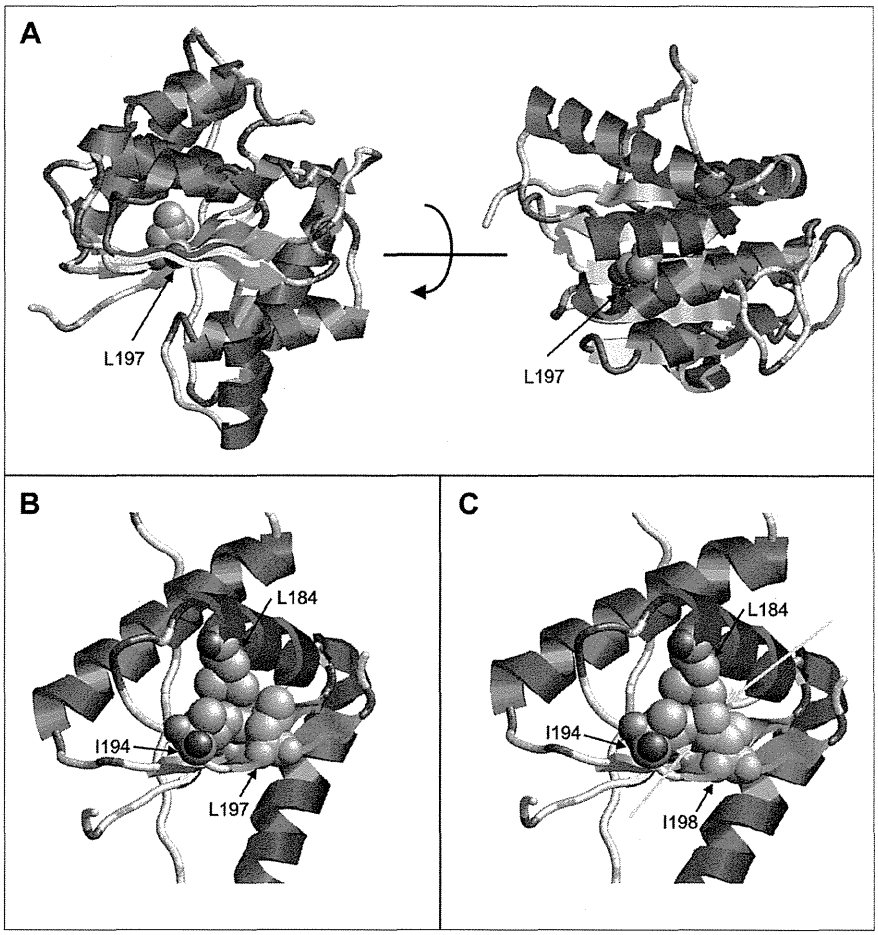

Figure 2. Molecular modeling of PGAP1. (A) Model of PGAP1 highlighting the position of Leu197. The two views differ by a rotation of 90° around the horizontal axis. (B) Interactions of Leu197 (green) with residues Leu184 and Ile194 of the hydrophobic core. (C) Interactions of Ile198 (green) in the Leu197del mutant. Clashes with the adjacent amino acids Leu184 and Ile194 are indicated by cyan arrows. Residues 203–316 are not shown in (B) and (C) for reasons of clarity.
doi:10.1371/journal.pgen.1004320.g002

since otocephaly and holoprosencephaly are not seen in some mouse strains [34,35].

Based on our mapping results, exome sequencing data and functional experiments that proved pathogenicity of the mutation, the previous reports on intellectual disability caused by mutations in the GPI synthesis pathway, and the mouse models that clearly show an association between the disruption of *Pgap1* and abnormalities of brain, we consider the deletion of leucine197 to be causative for the severe non-specific autosomal recessive intellectual disability in our examined patients of family MR079. *PGAP1* is the ninth gene of the GPI synthesis pathway that is now associated to a human phenotype (Table 1). Further mutations in *PGPA1* are needed to confirm our findings. Also, describing further patients with different mutations is necessary to delineate the phenotypes of the GPI deficiencies. For example, considering the defect in the modification of the GPI anchors, the alkaline phosphatase would not be elevated in patients with *PGAP1* mutations, but this needs to be confirmed.

In conclusion, null mutations in *PGAP1* lead to severe intellectual disability and encephalopathy with no obvious malformations; we add *PGAP1* to the growing number of genes involved in GPI-anchor deficiencies with human phenotypes. *PGAP1* deficiency causes a defect in the ER part of the GPI-AP biosynthesis that involves the remodeling of the anchors after attachment to proteins, and it leads to normal protein expression on the cell surface but to abnormal anchor structure.

Materials and Methods

The study was approved by the Ethic Committees of the Universities of Bonn and of Erlangen-Nürnberg in Germany, and Osaka University in Japan. Informed consent of all examined persons or of their guardians was obtained.

Mapping and exome sequencing

Genomic DNA was extracted from EDTA blood probes by standard methods and genotyped with the Affymetrix Mapping array 6.0 (Affymetrix, Santa Clara, CA, USA). Analysis did not reveal pathogenic deletions or duplications. Mendelian segregation was calculated using PedCheck software and was confirmed in all instances. Autozygosity mapping was performed using HomozygosityMapper [36]. DNA from individual III-3 was enriched using the